THESIS FOR THE DEGREE OF DOCTOR OF PHILOSOPHY

On the Control of Nematic Liquid Crystal Alignment

RASHA ATA ALLA

UNIVERSITY OF GOTHENBURG

Department of Physics
University of Gothenburg
Göteborg, Sweden, 2013

On the Control of Nematic Liquid Crystal Alignment

Rasha Ata Alla

ISBN: 978-91-628-8685-1

Doctorsavhandlingar vid Göteborg Universitet

Department of Physics
University of Gothenburg
SE-41296 Göteborg,
Sweden
Telephone +46(0)31 786 0000

Cover: Three bistable states displayed by one pixel liquid crystal device containing photoalignment layer with photo-patterned alignment in form of image (the photo in the middle). The image can be displayed only at special driving regime. Otherwise, the device displays only two bistable states: selectively reflecting state (green) or optically transparent state (black, since the cell has a black background). The device has whole non patterned electrode. The image is displayed due to the patterned alignment.
by Liquid Crystal Group, Department of Physics, University of Gothenburg, 2013.

Printed by Ale Tryckteam
Göteborg, Sweden 2013

ON THE CONTROL OF NEMATIC LIQUID CRYSTAL ALIGNMENT

RASHA ATA ALLA

Department of Physics
University of Gothenburg
Göteborg, Sweden, 2013

ABSTRACT

Liquid crystal displays (LCDs) are incorporated in a great variety of electronic devices such as laptops, mobile phones, TV sets, etc. The performance of LCDs depends strongly on the alignment of liquid crystal and therefore the reliable control of the alignment parameters, such as pretilt and anchoring strength, is of vital importance for the LCD industry. In this thesis are presented the results of the study of two categories of new alignment materials. The first category is composite photopolymerizable materials containing perfluorinated and siloxane units promoting uniform and thermally stable vertical alignment due to segregation and self-assembling of the fluorinated units. The performed study on the quality of the alignment, promoted by these materials at different relative concentrations of the components, and on their electro-optical characteristic and anchoring strength, showed that these materials are promising alignment materials which are good candidates to be employed in LCDs. The second category is two kinds of novel photoalignment materials. The study of these materials revealed the relationship between the molecular structure of the materials and their alignment ability, information which is very important for design of photoalignment materials for LCDs. Another study performed within this thesis revealed that the anchoring is not only a property of the solid surface, which is in contact with the liquid crystal, but also depends on the properties of the liquid crystal bulk such as ionic density, dielectric anisotropy and flexoelectric polarizability. This observation revealed the possibility for control of the anchoring properties and thus of the electro-optic characteristics of LCDs, in general, and of the response time, in particular. Important part of the thesis is devoted to study the necessary conditions for efficient control of the pretilt in LCDs. The results of this study confirmed unambiguously the conclusions derived in the recently suggested theoretical model describing the alignment transition from vertical to planar alignment in the case of presence of two alignment components - vertical and planar.

Keywords: liquid crystal alignment, nematic, photoalignment, anchoring energy, vertical, planar, pretilt, self assembling, azo

List of Publications

This thesis is based on the following publications:

I ***Composite Materials Containing Perfluorinated and Siloxane Units for Vertical Alignment of Liquid Crystals***, Rasha Ata Alla, Gurumurthy Hegde, Lachezar Komitov, Andrea Morelli, Emo Chiellini, Giancarlo Galli, *Soft Nanoscience Letters*, **3**, 11 (2013).

II ***Nano-Engineering of New Photoreactive Materials Having Fluorine Units: Synthesis and Photoalignment of Liquid Crystals***, Rasha Ata Alla, Gurumurthy Hegde, Arun M. Isloor, Boodappa Chandrakantha, Shridhar Malladi, M. M. Yusoff, and Lachezar Komitov, *Soft Nanoscience Letters*, **3**, 1 (2013).

III ***Azo Containing Thiophene Based Prop-2-enoates for Photoalignment of a Nematic Liquid Crystal***, Gurumurthy Hegde, Rasha Ata Alla , Avtar Matharu, Lachezar Komitov, accepted by *Journal of Materials Chemistry C*.

IV ***Thickness Dependence of The Anchoring Energy of a Nematic Cell***, R. M. S. Ataalla, G. Barbero, and L. Komitov, *Journal of Applied Physics* **113**, 164501 (2013).

V ***Light-control of Liquid Crystal Alignment from Vertical to Planar***, Rasha Ata Alla, Gurumurthy Hegde, and Lachezar Komitov, submitted for publication to *Applied Physics Letters*.

Contribution Report

The author has made the following contributions to the papers:

Paper I: Main author, all experimental work and manuscript preparation.

Paper II: Main author, all experimental work and contributed to manuscript preparation.

Paper III: Contributing author, contributed to the experimental work and manuscript preparation.

Paper IV: Main author, all experimental work, and contributed to theoretical analysis and manuscript preparation.

Paper V: Main author, all experimental, analysis work and manuscript preparation.

Contents

1 . Introduction

1.1 Liquid Crystalline State of Matter

Liquid crystals are organic materials consisting of molecules with anisotropic shape. The liquid crystal phase is an intermediate state of matter existing between crystalline (solid) and isotropic (liquid) phases. Liquid crystals have anisotropic physical properties like a solid but they flow like a liquid. This remarkable feature gave them unique properties and made them suitable for a number of applications such as liquid crystal displays (LCDs). The liquid crystal phase itself is divided into a number of sub-phases depending on the temperature or on the concentration of the molecules in a solution, as well as on the shape of the consisting molecules.
Thermotropic liquid crystal phases are formed between the crystalline and the isotropic phase by changing the temperature. Lyotropic liquid crystal phases can be obtained by changing the concentration of the organic molecules in the solution.
Liquid crystals are classified according to their molecules' shape. Calamitic liquid crystals consist of rod-like molecules and discotic liquid crystals their molecules' shape is disc-like. In general, the liquid crystal phase may have several sub-phases which are organized according to their degree of order between the most ordered phase of matter (solid) and the isotropic liquid phase.

The molecules in the liquid crystal have orientational order due to the molecular shape anisotropy. In high order liquid crystal phases the molecules may have in addition to the orientational order also a positional order. The nematic liquid crystals are the most important liquid crystal materials particularly for their device applications such as LCDs. In this thesis I treat the most simple phase among the liquid crystal phases: the nematic phase which consists of rod like molecules.
The nematic phase is the least order liquid crystalline phase among the liquid crystal thermotropic phases. It is characterized by a long-range orientational order of the rod-like molecules which do not have any positional order. Thus, the molecules are free to flow and the position of their center of mass is randomly distributed in the liquid crystal bulk as in a liquid, but the molecules still maintain their long-range directional order. Most nematics are uniaxial: they have one longer preferred axis, called the principal axis, and two perpendicular axes which are mutually perpendicular and equivalent.

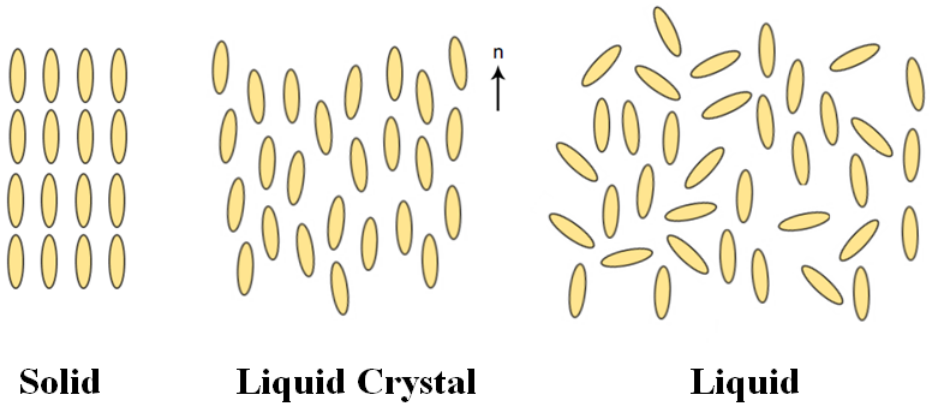

Figure 1.1: *The thermotropic Liquid crystal phase, an intermediate phase of matter between the solid and liquid phases.*

1.1.1 Director and Order Parameter

The preferred orientation direction of the liquid crystal molecules is represented by a direction along which the molecules are oriented. The preferred direction of the molecular long axis is defined by a non-polar unit vector **n** called the director. In nematics **n** is equivalent to -**n** due to existing mirror symmetry of the nematic phase. The orientational order of nematics is described by a second rank symmetric traceless tensor. The degree of order is specified by an order parameter S represented by the average of the second Legendre polynomial [1]

$$S = \langle P_2(\cos\theta)\rangle = \frac{1}{2}\langle 3\cos^2\theta - 1\rangle, \tag{1.1}$$

θ is the angle between the molecular long axis and the director **n**, and the brackets indicate an average over all the molecules in the liquid crystal. The liquid crystal order parameter is a scalar varying in the interval $(0 < S < 1)$ where 0 and 1 represents isotropic state and perfectly ordered state, respectively.

1.2 Anisotropic Physical Properties

An important consequence of the anisotropic shape of liquid crystal molecules is their anisotropic physical properties. In nematics each measured physical property will have two different values depending on the direction of the measurement: parallel or perpendicular to the principal axis given by the director because of the uniaxial symmetry of liquid crystal molecules.

1.2.1 Dielectric Anisotropy

Due to the anisotropy of the liquid crystals' molecular structure their response to an applied electric field may be different depending on the dielectric anisotropy of the liquid crystal material. The nematic liquid crystals possess two different values of the dielectric constants: ($\varepsilon_{\parallel}$) - for a field oscillating parallel to the optical axis and ($\varepsilon_{\perp}$) for a field oscillating perpendicular to it (fig.(1.2)). The dielectric properties for nematics are represent by dielectric tensor $\overline{\varepsilon}$ which has a diagonal form

$$\overline{\varepsilon} = \begin{pmatrix} \varepsilon_{\perp} & 0 & 0 \\ 0 & \varepsilon_{\perp} & 0 \\ 0 & 0 & \varepsilon_{\parallel} \end{pmatrix}. \tag{1.2}$$

The dielectric anisotropy then is written as [1]

$$\Delta\varepsilon = \varepsilon_{\parallel} - \varepsilon_{\perp}. \tag{1.3}$$

A molecule with positive dielectric anisotropy ($\varepsilon_{\parallel} > \varepsilon_{\perp}$) will have the greater polariz-

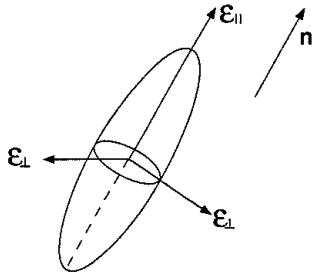

Figure 1.2: *Parallel and perpendicular components of the dielectric constant for uniaxial molecule*

ability along the molecule long axis (coinciding with the molecule optical axis), while for the one with negative dielectric anisotropy ($\varepsilon_{\parallel} < \varepsilon_{\perp}$) the greater polarizability will be perpendicular to it. Thus the sign of the dielectric anisotropy will define whether the nematic molecule will lie along the direction of the applied electric field or perpendicular to it (c.f. fig.(1.3)). For an arbitrary direction of the electric field $\mathbf{E}$ the relation between it and the electric displacement $\mathbf{D}$ has the form [2]

$$\mathbf{D} = \varepsilon_{\perp}\mathbf{E} + (\varepsilon_{\parallel} + \varepsilon_{\perp})(\mathbf{n}\cdot\mathbf{E})\mathbf{n}. \tag{1.4}$$

The electric contribution to the free energy density will be

$$f_E = -\int \mathbf{D}.d\mathbf{E} = -\frac{1}{2}\left(\varepsilon_{\perp}E^2 + \Delta\varepsilon(\mathbf{n}\cdot\mathbf{E})^2\right), \tag{1.5}$$

where the second term is the one which depends on the field orientation and it favors alignment of the liquid crystal parallel to the field, for positive dielectric anisotropy, and perpendicular to the field for negative dielectric anisotropy.

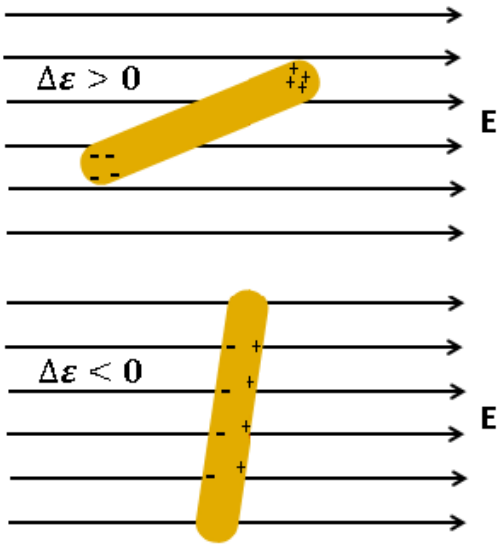

Figure 1.3: *Orientation of Liquid crystal molecules with positive and negative dielectric anisotropy as a response to the applied electric field.*

1.2.2 Optical Anisotropy

The optical properties of liquid crystals vary with direction. In the case of uniaxial liquid crystals, such as nematics, there are two refractive indices. The ordinary refractive index ($n_\circ$) is measured when the polarization direction of the incident light perpendicular to the optical axis. The extraordinary refractive index (n_e) is measured when the polarization direction of the incident light parallel to the optical axis. The birefringence (i.e. optical anisotropy) of liquid crystals represents the difference between the two refractive indices; the extraordinary and the ordinary index, expressed as

$$\Delta n = n_e - n_\circ \tag{1.6}$$

When the incident wave propagates in a tilted direction to the optical axis (as illustrated in fig.(1.4)) the refractive index of the ordinary wave will have the same value $n_\circ$ but the refractive index for the extraordinary wave n_e will have an effective value according to [3]

$$n_{eff} = \frac{n_e n_\circ}{\sqrt{n_e^2 \cos^2\vartheta + n_\circ^2 \sin^2\vartheta}}, \tag{1.7}$$

where ϑ is the angle between the optical axis and the light propagation direction. In this situation the birefringence will be

$$\Delta n = n_{eff} - n_\circ. \tag{1.8}$$

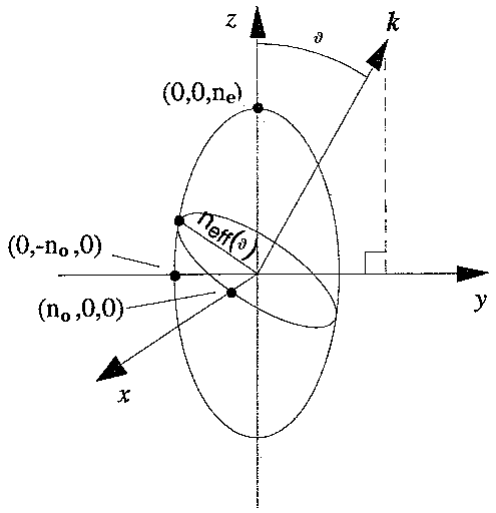

Figure 1.4: *The index ellipsoid for an uniaxial material.*

1.3 Liquid Crystal/Solid Surface Interactions

Liquid crystals attracted the interest of scientists and engineers due to their anisotropic physical properties and the easy control of their orientation by external fields such as magnetic, electric and light. In order to make use of the anisotropic physical properties of the nematic liquid crystals they have first to be aligned uniformly with the long molecular axis oriented along a preferred direction. Such uniform alignment of the liquid crystal molecules can be achieved by applying an external field: magnetic, electric or light, as well as by the interaction of the liquid crystal with a solid surface.

Since the liquid crystal is a liquid which easily flows, in order to be studied and used practically, in displays for instance, the liquid crystal material is enclosed in between two solid substrates in so called sandwich geometry. The cell gap usually is of several micrometers in size and the solid substrates are glass plates which may bear transparent electrodes on the inner surface of both or only on one of the substrates. The interaction of the liquid crystal molecules with the solid substrates' surface will influence the liquid crystal in contact with this surface [4].

Liquid crystal molecules in the interfacial layer will be in a different environment compared to the rest of the liquid crystal molecules so they will feel different molecular interactions and hence they will adopt unique properties different from the properties of the entire bulk liquid crystal. The physical properties of the interface layer change continuously with the distance from the interface to the bulk in both absolute value and direction [3]. Both the director and the order parameter will be affected by the existence of the two solid surfaces and this influence will be transferred through the bulk via elastic forces.

In fact, the small thickness of the sandwiched cell gap as well as the relatively large

area of the surfaces enhance the role of the liquid crystal-surface interaction on the bulk properties. The impact of the liquid crystal/solid surface interaction on the liquid crystal bulk properties is often used to align liquid crystal molecules to specific desired direction without applying any external field such as an electric field, for instance. This is usually done by generating some kind of anisotropy of the surface physical properties.

1.3.1 Liquid Crystals Alignment

Liquid crystal alignment is a very important factor in almost all liquid crystal device applications. In general, liquid crystal molecules can be aligned by the solid substrate surfaces. The balance between the liquid crystal surface tension γ_L and the solid surface tension γ_S, when a droplet of liquid crystal is placed on a solid surface, will determine which direction liquid crystal molecules will prefer to adopt. The elongated molecules will choose to order themselves perpendicular to the surface, if $\gamma_L > \gamma_S$, in order to minimize the surface energy since in this case the intermolecular forces between liquid crystal molecules dominate. The forces across the surface will dominate, when $\gamma_L < \gamma_S$,

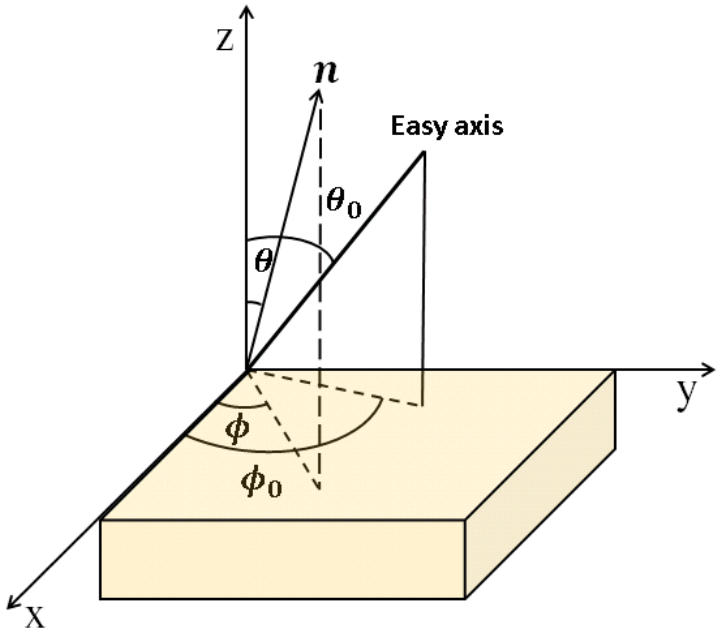

Figure 1.5: *Director orientation and easy axis direction at the interface to the substrate surface.*

and the molecules will align themselves parallel to the surface [5]. For the third case when $\gamma_L \approx \gamma_S$ the molecules will adopt a tilted alignment.
The type of alignment at the surface is defined by the director which is specified by the surface polar angle θ and the azimuthal angle ϕ, see fig.(1.5). At thermal equilibrium, to minimize the surface energy, the director is aligned towards a preferred direction which is

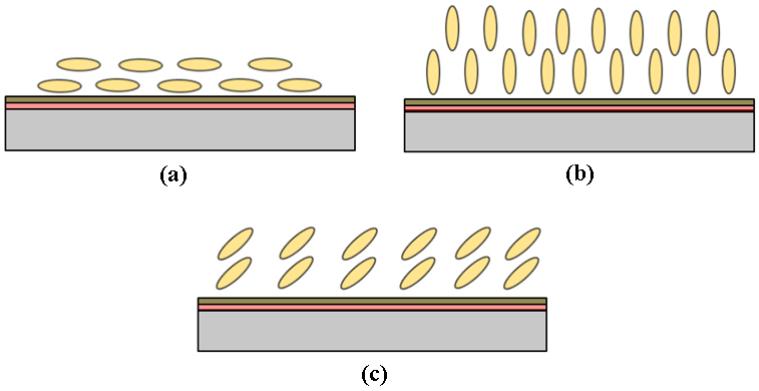

Figure 1.6: *Fundamental liquid crystal alignments on substrates surfaces: (a) Planar (b) Homeotropic (c) Tilted.*

called the easy axis $(\theta_\circ, \phi_\circ)$. Basically Liquid crystal alignment is classified according to the easy axis orientation to either homeotropic (vertical), planar or tilted alignment (see fig.(1.6)). In homeotropic alignment liquid crystal molecules are aligned perpendicular to the surface with $\theta_\circ = 0°$ and $\phi_\circ$ is arbitrary or fixed. The planar alignment, where the easy axis is parallel to the surface, is divided to uniform planar with $\theta_\circ = 90°$ and $\phi_\circ$ fixed, and degenerate planar with $\theta_\circ = 90°$ and $\phi_\circ$ is arbitrary. The tilted alignment has a polar angle $\theta_\circ$ which has fixed value between $0°$ and $90°$.

1.4 Continuum Theory

In a nematic liquid crystal cell the liquid crystal molecules adopt a certain alignment promoted by their interactions with the solid wall. Well aligned liquid crystal medium is defined by assuming that the direction of the director is almost uniform through the medium i.e. independent of the position. Let us call this state of uniformity the equilibrium state which is the state of the lowest energy. If the cell substrates promote different alignment of the liquid crystal enclosed in between them then the orientation of the director across the liquid crystal layer will no longer be with a constant orientation. The director orientation will change continuously across the liquid crystal layer. This continuous change is called elastic deformation and it leads to an increase of the energy of the system. The free energy density of this distorted medium can be expressed as a sum of the undistorted energy density $(f_\circ)$ and the Frank elastic free energy density which is the free energy density due to the bulk distortion (f_d)

$$f(\mathbf{r}) = f_\circ + f_d(\mathbf{r}). \tag{1.9}$$

It was found that the Frank energy density is given by [1]

$$f_d(\mathbf{r}) = \frac{1}{2}\{k_{11}[\nabla.\mathbf{n}(\mathbf{r})]^2 + k_{22}[\mathbf{n}(\mathbf{r}).\nabla \times \mathbf{n}(\mathbf{r})]^2 + k_{33}[\mathbf{n}(\mathbf{r}) \times \nabla \times \mathbf{n}(\mathbf{r})]^2\}. \tag{1.10}$$

The constants k_{11}, k_{22} and k_{33} are the elastic constants for splay, twist and bend, respectively (c.f. fig.(1.7)), and they are called Frank elastic constants. Frank elastic constants

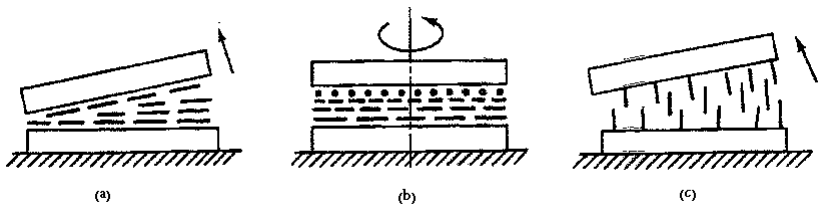

Figure 1.7: *Distortions in nematic liquid crystal cell: (a) splay (b) twist (c) bend [6].*

describe the elastic properties of the medium. They describe the stiffness of the liquid crystal respond with respect to the distortions. One-elastic constant approximation is used, in some cases, for practical reasons i.e.

$$k_{11} = k_{22} = k_{33} = k.$$

Equation (1.10) can be rewritten in simpler form

$$f_d(\mathbf{r}) = \frac{k}{2}\{[\nabla.\mathbf{n}(\mathbf{r})]^2 + [\nabla \times \mathbf{n}(\mathbf{r})]^2\}. \tag{1.11}$$

The application of external fields, such as electric and magnetic fields, to the cell implies to add the fields contributions to the total free energy density

$$f = f_d + f_E + f_M. \tag{1.12}$$

The total free energy of the sample is given by

$$F = \int_v f d^3r, \tag{1.13}$$

where v is the volume of the sample. The equilibrium alignment of the director through the cell will be found by minimizing the total free energy by solving the corresponding Euler-Lagrange equation for the bulk distortion [7]

$$\frac{\partial f}{\partial \theta} - \frac{d}{dz}\left[\frac{\partial f}{\partial \acute{\theta}}\right] = 0 \qquad \text{and} \qquad \frac{\partial f}{\partial \phi} - \frac{d}{dz}\left[\frac{\partial f}{\partial \acute{\phi}}\right] = 0, \tag{1.14}$$

with boundary conditions

$$\pm\left[\frac{\partial f}{\partial \acute{\theta}}\right] = 0, \qquad \pm\left[\frac{\partial f}{\partial \acute{\phi}}\right] = 0, \tag{1.15}$$

where $\theta(z)$ and $\phi(z)$ are the polar and azimuthal angles (c.f. fig.(1.5)), $\acute{\theta} = \partial\theta/\partial z$, and $\acute{\phi} = \partial\phi/\partial z$.

1.5 Anchoring Strength

Liquid crystal molecules which are adjacent to the surface will feel molecular interactions quite different from those in the liquid crystal bulk. This difference will result in an increase of the energy in the surface layer. The free surface energy of nematic liquid crystals includes two parts: isotropic and anisotropic. The isotropic part is the surface tension which determines which direction the director will adopt. The anisotropic part, which is the anchoring energy, represents the amount of energy needed to deflect the director from the equilibrium position i.e. the easy axis direction; thus the surface free energy F_s will be [8]

$$F_s = F_s^i + F_s^a, \tag{1.16}$$

where F_s^i and F_s^a are the isotropic and anisotropic parts, respectively. For a nematic liquid crystal cell the total free energy will be [8]

$$F = F_\circ + \int_v f d^3r + F_{s1} + F_{s2}, \tag{1.17}$$

where $F_\circ$ includes both surface and bulk isotropic parts, f represents either Frank elastic energy density (i.e. f_d) or the total free energy density for the bulk distortion (c.f. equation (1.12)), F_{s1} and F_{s2} are the two surfaces energies.
The simplest way to express the anisotropic part of the surface energy is the one which was suggested by Rapini-Papoular as a function of the nematic bulk orientational azimuthal (ϕ) or polar (θ) surface angles [8]

$$F_s^a(\theta) = \frac{1}{2} w^\theta \sin^2(\theta - \theta_\circ^s), \tag{1.18}$$

$$F_s^a(\phi) = \frac{1}{2} w^\phi \sin^2(\phi - \phi_\circ^s), \tag{1.19}$$

where w^θ (related to the deviation of the director from the normal to the substrate) and w^ϕ (related to the deviation of the director in the plane of the substrate) are the polar and azimuthal anchoring strength, respectively. $\theta_\circ^s$ and $\phi_\circ^s$ are the polar and azimuthal anchoring orientations given by the surface. As mentioned in section 1.4, to find the equilibrium alignment of the director through the cell, the energy density should be minimized by solving equation (1.14). The boundary conditions equation (1.15) will include the two surfaces contributions

$$-\left[\frac{\partial f}{\partial \acute{\theta}}\right]_1 + \frac{\partial f_{s1}}{\partial \theta_1} = 0, \quad -\left[\frac{\partial f}{\partial \acute{\phi}}\right]_1 + \frac{\partial f_{s1}}{\partial \phi_1} = 0, \tag{1.20}$$

$$\left[\frac{\partial f}{\partial \acute{\theta}}\right]_2 + \frac{\partial f_{s2}}{\partial \theta_2} = 0, \qquad \left[\frac{\partial f}{\partial \acute{\phi}}\right]_2 + \frac{\partial f_{s2}}{\partial \phi_2} = 0. \tag{1.21}$$

where the indices 1 and 2 refer to the upper and lower surfaces. The boundary equations describe the balance between the bulk elastic torque and the surfaces energies.

1.5.1 Polar Anchoring Strength

For a homeotropic or planar nematic cell, where we consider only the polar anchoring energy ($w^{\vartheta} = w$), in a cell with two limiting surfaces (located at $z = \pm d/2$) with similar conditions equation (1.17), the total free energy will have the form

$$F = \frac{k}{2} \int_{-d/2}^{+d/2} dz \left[\frac{d\theta(z)}{dz} \right]^2 + w\theta^2, \tag{1.22}$$

The Rapini-Papoular approximation for small angle θ: $\sin\theta \approx \theta$ have been used. The corresponding Euler-Lagrange equation for the bulk distortion is

$$\frac{\partial^2 \theta(z)}{\partial z^2} = 0, \tag{1.23}$$

and the boundary condition equation using equations (1.20) and (1.22) will be

$$w\theta - k\frac{\partial \theta}{\partial z} = 0. \tag{1.24}$$

The general solution of Euler-Lagrange equation for the bulk (equation (1.23)) will give $\theta(z) = Az + B$, taking equation (1.24) into consideration, we get

$$\theta(z) = \frac{w^{\theta}}{2k + wd}(z + k/w). \tag{1.25}$$

Let $\theta = 0$ for strong anchoring

$$b = |z| = \frac{k}{w}, \tag{1.26}$$

where b which have the dimension of length and is called the extrapolation length. The extrapolation length is considered as a measure of the anchoring strength.

1.5.2 The Effective Anchoring Strength

The solid surface is characterized by an easy direction $\mathbf{n}_{\circ}$ and an anchoring strength w. Both of them are assumed to arise from the liquid crystal/ solid surface interactions. The anisotropic part of the surface energy for a homeotropic nematic liquid crystal cell may rewritten as

$$F_s = -\frac{1}{2} w \cos^2 \alpha, \tag{1.27}$$

where $\alpha = \cos^{-1}(\mathbf{n}_{\circ} \cdot \mathbf{n})$ represents small deviation from the easy axis (see fig.(1.5)).
It was observed previously that for a nematic liquid crystal confined between two substrates, the inner surfaces of the substrates selectively adsorb the ions contained in the liquid crystal [9,10]. The selective adsorption of ions creates a surface electric field normal to the surface. This electric field extends to the bulk over Debye screening length λ_D and it can approximately given by [11]

$$E_s(z) = (\sigma/\varepsilon) \exp(-z/\lambda_D), \tag{1.28}$$

$\varepsilon = (\varepsilon_{\parallel} + 2\varepsilon_{\perp})/3$ is the average dielectric constant. The surface density of the electric charges, σ, depends on the cell gap thickness as [10]

$$\sigma = \Sigma \frac{d}{d + 2\lambda_D}, \tag{1.29}$$

where Σ is a material property which depends on the conductivity of the liquid crystals. The surface field has an orienting effect on nematic liquid crystals through the coupling to the dielectric anisotropy $\Delta\varepsilon$. The dielectric energy density then is given by

$$f_{el} = -\frac{1}{2}\Delta\varepsilon \left(\mathbf{n}.\mathbf{E_s}\right)^2. \tag{1.30}$$

The dielectric contribution to the surface energy can be calculated by integrating equation (1.30) from 0 to ∞ and substituting equation (1.28) to get

$$F_{el} = \int_0^{\infty} f_{el}\, dz = -\frac{1}{4}\Delta\varepsilon \left[\frac{\sigma}{\varepsilon}\right]^2 \lambda_D \cos^2\alpha. \tag{1.31}$$

The distortion of nematic liquid crystal uniform alignment near the surface will induce flexoelectric polarization which will contribute to the effective surface energy by the term [11]

$$F_A = -e\frac{\sigma}{\varepsilon}\cos^2\alpha, \tag{1.32}$$

where $e = e_{11} + e_{33}$ is the average flexoelectric coefficient [2]. The effective surface energy will contain three terms; equations given by (1.27),(1.31) and (1.32), namely

$$F_{eff} = F_s + F_{el} + F_A. \tag{1.33}$$

Equation (1.33) for the total effective surface energy may be rewritten in this form

$$F_{eff} = -\frac{1}{2}w_{eff}\cos^2\alpha, \tag{1.34}$$

where the effective anchoring strength w_{eff} has the form

$$w_{eff} = w + \frac{\sigma}{\varepsilon}\left(\frac{\Delta\varepsilon}{2\varepsilon}\lambda_D\,\sigma + 2\,e\right). \tag{1.35}$$

1.6 Frederick Transition

Applying an external field such as electric field across a cell containing a nematic liquid crystal with positive dielectric anisotropy and initial field-off planar alignment, will re-orient the molecules in the bulk of liquid crystal layer towards the applied field. Similar field-induced re-orientation of the liquid crystal molecules takes place in a nematic liquid crystal layer with negative dielectric anisotropy and initial field-off homeotropic alignment. This phenomenon is called a Frederick transition and it takes place when the value

Figure 1.8: *Frederick transition in a homeotropic nematic cell with negative dielectric anisotropy.*

of the applied field exceeds a minimum so-called threshold field.

The total free energy, for each one of the previously mentioned situations when an electric field is applied across the cell parallel to the z-axis, will have the form (see fig.(1.5))

$$F = \frac{1}{2}\int_0^d dz \left[k_{ii} \left(\frac{d\theta(z)}{dz} \right)^2 - |\Delta\varepsilon| E^2 \sin^2\theta(z) \right] + \frac{1}{2} w_1 \sin^2\theta_1 + \frac{1}{2} w_2 \sin^2\theta_2, \qquad (1.36)$$

where $k_{ii} = k_{22}$ is the splay elastic constant and $k_{ii} = k_{33}$ is the bend elastic constant. w_1 and w_2 is the anchoring strength for the first and the second substrates' surface, respectively. The deflection angles at the two surfaces are $\theta_1 = \theta(0)$, $\theta_2 = \theta(d)$, where d is the cell thickness, and E is the amplitude of the applied electric field.

Minimizing equation (1.36), in the limit of small distortions $\theta \approx \sin\theta$ and constant electric field, we obtain the equilibrium equation for the bulk distribution of the director

$$\frac{d^2\theta(z)}{d\,z^2} + q^2\theta = 0, \qquad (1.37)$$

with boundary conditions

$$-\,k_{ii}\frac{d\theta(z)}{dz} + w_1\theta_1 = 0, \qquad z = 0, \qquad (1.38)$$

$$k_{ii}\frac{d\theta(z)}{dz} + w_2\theta_2 = 0, \qquad z = d. \qquad (1.39)$$

The solution of equation (1.37) is

$$\theta(z) = a\sin(q\,z) + b\cos(q\,z), \qquad (1.40)$$

where $q = E\sqrt{|\Delta\varepsilon|/k_{ii}}$ has the dimensions of an inverse length, and its inverse; q^{-1} represents the coherence length which is the distance from the solid substrate at which the nematic director will be completely reoriented by the electric field. Using equation(1.40) for the first surface we find that $\theta(0) = b$, and

$$\frac{d\theta(0)}{dz} = q\,a \qquad (1.41)$$

Using $\theta(0) = b$ and equation (1.41) in equation (1.38) to obtain one equation for a and b

$$\frac{a}{b} = \frac{w}{q\,k_{ii}}. \tag{1.42}$$

If the two limiting surfaces are identical i.e. the initial surface conditions are symmetric, hence the deformation induced by the applied electric field should be also symmetric and have maximum value at the middle of the cell at z = $d/2$ (see fig.(1.8)).

$$\frac{d\theta}{dz}(d/2) = a\,q\cos(q\,z) - b\,q\sin(q\,z) = 0. \tag{1.43}$$

Thus we get

$$\frac{a}{b} = \tan(q\,d/2). \tag{1.44}$$

Combining equation(1.42) and (1.44) we get an expression for the anchoring strength

$$w = q\,k_{ii}\tan(q\,d/2). \tag{1.45}$$

In the limit of strong anchoring $w \longrightarrow \infty$ there is no deformation on the surfaces i.e. $\theta(0) = \theta(d) = 0$, then using equation(1.40)

$$\theta(0) = 0 \longrightarrow b = 0, \tag{1.46}$$

$$\theta(d) = 0 \longrightarrow a\sin(q\,d) = 0. \tag{1.47}$$

Equation (1.47) implies that $q = \pi/d$ which gives the minimum field needed to cause the distortion, i.e. the threshold field

$$E_t = \frac{\pi}{d}\sqrt{\frac{k_{ii}}{|\Delta\varepsilon|}}. \tag{1.48}$$

1.7 Electro-optic Response

Liquid crystal materials are considered as an electro-optic medium since its optical properties can be controlled by applying an electric field. The orientation of liquid crystal molecules and hence the birefringence of the sandwich cell containing the liquid crystals can be controlled by the applied electric field. The materials with birefringence which could be controlled by applying electric field are useful in manufacturing electrically controllable optical devices such as wave retarders and intensity modulators. The light which passes through a slab of nematic liquid crystal cell, with thickness d, placed between two crossed polarizers will experience a phase difference between the ordinary and extraordinary ray expressed as

$$\delta = \frac{2\pi}{\lambda}(n_e - n_\circ)d, \tag{1.49}$$

where λ is the light wavelength. The transmitted intensity will be

$$I = I_\circ \sin^2 2\psi \sin^2 \frac{\delta}{2}, \tag{1.50}$$

where $I_\circ$ is the intensity of the incident polarized light, and ψ is the angle between the optical axis and the analyzer.
The operation of nematic liquid crystal cells, when an electric field is applied across them parallel to the z-axis, is governed by the balance between elastic and viscous torques and the electric torque. This balance can be expressed as

$$k\frac{d^2\theta}{dz^2} + E^2\Delta\varepsilon \sin\theta\cos\theta = \eta\frac{\partial\theta}{\partial t}, \tag{1.51}$$

where θ is the polar angle, and η is the rotational viscosity. Applying constant electric field for strong vertical cell ($\theta = 0°$) with negative anisotropy liquid crystal or for a planar cell ($\theta = 90°$) with positive anisotropy liquid crystal, in the limit of small distortions, the initial condition is the maintained below a critical field or voltage

$$V_c = \pi\left[\frac{k}{\Delta\varepsilon}\right]^{\frac{1}{2}}. \tag{1.52}$$

The critical voltage is the value above which the medium deforms and $\theta(z)$ changes. For vertical and planar alignment, respectively, without any pretilt, the applied voltage induces a molecular tilt which is degenerate and results in domains formation which deteriorates the LCD performance. Introducing a very small tilt in the cell is sufficient to avoid the domains. From equation (1.51) an approximate expressions was found for the switch on time (i.e. rise time: τ_r) and the switch off (decay) time τ_d [12]

$$\tau_r = \frac{\eta d^2}{(\Delta\varepsilon V^2 - k\pi^2)}, \tag{1.53}$$

$$\tau_d = \frac{\eta d^2}{k\pi^2}. \tag{1.54}$$

The above equations for rise and decay time are applicable for cells with strong boundary conditions.

2 . Liquid Crystals Alignment Techniques

Concerning the control of the liquid crystal alignment by means of substrate surface treatment there are different treatment methods for achieving such a control. Any one of these methods has its advantages and disadvantages and what is suitable for some materials or applications may not be suitable for an other. In fact it is quiet important for almost all liquid crystal device applications to have a reliable control on the liquid crystal alignment by a feasible technique without applying external field. The key factor in the surface alignment is the interactions between the surface and liquid crystal molecules. Steric forces which according to pauli's exclusion principle prevent different molecules from penetrating each other will result in certain type of alignment. In fact, the liquid crystal/ solid surface interaction is complex interaction including, for instance, Van der Waals forces, dipole-dipole interactions, hydrogen bounding, and chemical bounding.
The focus in this chapter will be on liquid crystal alignment techniques in general.

2.1 Rubbing Technique

Mechanical rubbing of the substrate surface is the oldest method for creating anisotropy of the surface physical properties which in turn will promote certain alignment of the liquid crystal molecules in contact with this surface. According to the rubbing method the glass substrate surface is simply rubbed unidirectionally by means of a piece of special type of cloth either by hand or by a rubbing machine. Such a machine consists of a roller covered by rubbing cloth and a platform to hold the substrate and moving in one direction. Either the roller or the substrates stage moves at a constant speed. The distance between the roller and the stage is also adjustable to control the pile imprint. The rubbing strength is important factor for the characteristics of the obtained liquid crystal alignment.
Commonly the glass substrate is covered by an alignment material such as polyimide, for instance, before being imposed to the rubbing process. The rubbing process cause a local heating and stretching of the alignment layer, which causes alignment of the main chain of the polyimide as well as it generates grooves in the direction of the rubbing [13, 14]. The liquid crystal molecules, and thus the director, prefer to lie parallel to the rubbing direction in order to minimize the surface energy. By using the rubbing technique it is possible to get planar or tilted alignment depending on the properties of the alignment

material and the rubbing strength [15–18]. As a contact alignment method, the rubbing alignment technique is simple but it has many disadvantages such as mechanical defects, surface charges and is not applicable for achieving of patterned alignment layers, necessary for different device applications.

2.2 Oblique Evaporation Technique

In this non-contact technique the surface of the glass substrate is bombarded by an evaporation beam of some oxides, such as SiO and GeO, at specific incident angle [19]. The value of the incident angle of evaporation as well as the other evaporation parameters such as temperature, pressure, etc. control the surface structure and thus the imposed alignment on the liquid crystal in contact with the evaporated film. For example, by evaporating at an angle of about 30° with respect to the substrate normal, uniform planar alignment could be achieved with 0° tilt, while evaporating at an angle of 80° results in tilted alignment [20].

2.3 Physico-chemical Technique

Liquid crystal alignment can be achieved by using surface coupling agents. Surface coupling agents are used either by depositing them on top of the glass substrate or by mixing them with the liquid crystal material. The main mechanisms which rule this technique are steric forces and polar interactions. Surface coupling agents have two parts, where one of them is hydrophilic and the other hydrophobic. They give either homeotropic or planar alignment, when deposited on the inner substrate surface, depending on their specific properties and the surface density of the agents. For instance, the surfactant lecithin and HTAB (Hexadecyl Trimethyl Ammonium Bromide) as well as some polyimides having alkyl chains as side groups are used for promoting homeotropic alignment [21–24]. Langmuir- Blodgett films of surfactants transferred on the substrate surface could effectively promote homeotropic alignment, as well.

2.3.1 Photopolymerizable Self-assembled Materials

In the present thesis, new series of composite photopolymerizable self- assembled materials prepared mainly from perfluorinated and polysiloxane groups suitable for homeotropic alignment were studied extensively. The chemical structures for the different components are illustrated in fig.(2.1).

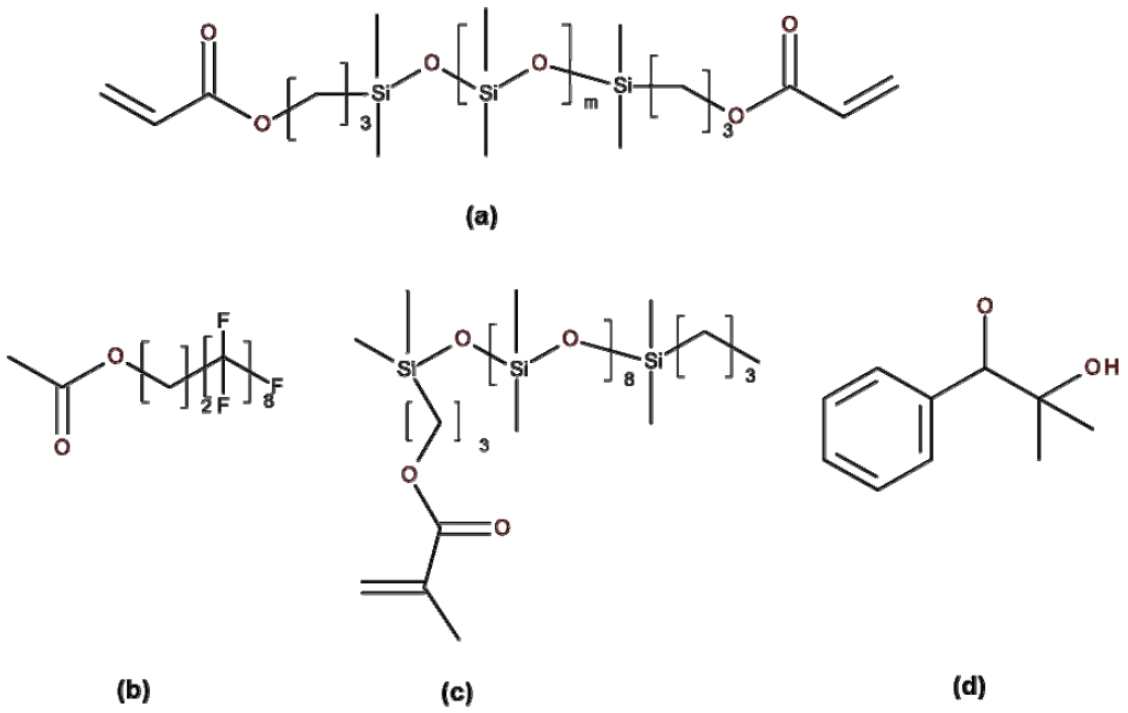

Figure 2.1: *Compounds used of the composite alignment materials: polysiloxane crosslinker (a), perfluorinated (b) and polysiloxane units (c) and photointiator (d).*

2.3.2 Experimental Procedure

The materials under study are composite materials contain several components. The components are: polysiloxane crosslinker, perfluorinated and polysiloxane units, and photointiator. The materials have been dissolved in polyglycol methyl ether acetate (PGMEA). Four different mixtures have been prepared using different ratios of the components (c.f. Table 2.1). Thin films of the material under study deposited (spin coated) on top of the

Table 2.1: *Alignment materials composition.*

Composite alignment material	Components			
	a wt%	b wt%	c wt%	d wt%
Mixture 1	83	15	-	2
Mixture 2	54	6	39	1
Mixture 3	53	16	29	2
Mixture 4	-	89	8	3

inner surface of each substrate (c.f. section 5.1). The coated substrates then baked at $100°C$ for 15 min to evaporate the solvent. UV photopolymerization was carried out at room temperature by normal incident of a non-polarized UV light at an energy level of

about 20 mJ/cm^2 for different exposure times. Two substrates were assembled together to form one cell. The cell gap thickness measured using the procedure described in section 5.2. Nematic liquid crystal MLC 6608 ($\Delta\varepsilon < 0$) (Merck) was injected into the cells at isotropic temperature. A reference cell with alignment layer prepared from SE1211 (Nissan Chem.) was assembled for comparison. Electro-optics measurements carried out as described in section 5.4.

2.3.3 Results and Discussion

Very good and uniform vertical alignment was found in the assembled cells at 20 min exposure time. The polar anchoring energy w was calculated assuming finite (weak) anchoring strength using the approximation [25]

$$\tau_{off} \approx \frac{4\gamma_1 d}{w\pi^2}, \tag{2.1}$$

where τ_{off} is the decay time, γ_1 is the rotational viscosity, d is the cell gap thickness, and w is the polar anchoring energy. The measured response times and the calculated anchoring energy was found to give different values according to the relative ratios of the components of the material under study (c.f. Table 2.2).

As mentioned previously, the liquid crystal/ solid surface interaction is the key factor

Table 2.2: *Fall τ_{off} and rise τ_{on} time, and polar anchoring energy w.*

Composite alignment material	τ_{off} ms	τ_{on} ms	d/τ_{off} $\times 10^{-3} m/s$	w $J/m^2 \times 10^{-5}$
Mixture 1	10	38	0.320	2.4
Mixture 2	14	24	0.264	2
Mixture 3	12	32	0.283	2.2
Mixture 4	22	60	0.205	1.5
Ref. material SE1211	8.82	9.36	0.453	2.17

in the achievement of a desirable kind of liquid crystal alignment. This interaction is complex and involved a number of components. The interplay between these components results in certain type of alignment which characteristics depend on the nature of the components. Therefore, by controlling the number of components involved in the liquid crystal/ surface interactions and their interplay we can control the liquid crystal alignment and its characteristics.

This unique combination of perfluorinated groups and polysiloxane units gives rise to excellent uniform homeotropic alignment with suitable thermal stability and good anchoring energy. As mentioned in the first chapter the balance between the liquid crystal surface tension and the solid surface tension determines the type of the alignment. Moreover,

the steric interactions between the liquid crystal molecules and side groups with shape anisotropy, properly anchored to the substrate surface, will contribute for the achievement of homeotropic alignment of the liquid crystal.
Thus the key factors in this composite material, found to promote homeotropic alignment, are the low surface energy due to the polysiloxane as well as of the fluorinated groups besides the steric interactions between the self-assembled fluorinated groups and liquid crystal molecules. Due to the low surface energy the fluorinated side groups are self-segregated in nano-size domains with their long axis making an angle of about 45° between them. This gives enough space in between the fluorinated groups for penetration of a number of liquid crystal molecules.
Electro-optic measurements besides the polar anchoring energy calculations, considering finite (weak) anchoring condition showed promising strong polar anchoring besides the crucial importance of the relative concentrations of polysiloxane and perfluorinated compounds on the properties of the alignment layers made from these materials. These novel photopolymerizable self-assembled alignment material showed promising strong polar anchoring in addition to the excellent quality of the achieved homeotropic alignment. It should be noted that the characteristics of the homeotropic alignment promoted by the alignment layer made from this composite material dependent strongly on the relative concentrations of polysiloxane and perfluorinated compounds.

2.4 Photoalignment Technique

The photoalignment technique is a modern feasible approach for the achievement of high quality liquid crystal alignment. It was brought to light since 1991 when it was demonstrated that liquid crystal alignment can be achieved by exposing a surface of azobenzene-mixed polyimide to linearly polarized UV light [26]. During the last decade a variety of materials and different photoaligning techniques have been proposed and developed.

The photoalignment effect is obtained by illuminating a thin film of photoresponsive material by linearly polarized UV light, it was found to induce an anisotropic chemical reaction and thus generating anisotropy of the physical properties of the alignment layer and, hence, of its contact surface with the liquid crystal (see fig.(2.2)). The anisotropic absorption of the exciting linearly polarized UV light by the photoresponsive molecules of the alignment material is the effect behind their anisotropic orientational distribution created by the UV light. After filling liquid crystal into the cell gap, the intermolecular interactions between the liquid crystal molecules and the interaction with the aligning surface should be strong enough to orient liquid crystal molecules towards the desired direction. Liquid crystal alignment will be depending on the structure of the liquid crystal molecules and on the nature of the photoalignment material as well as on their interac-

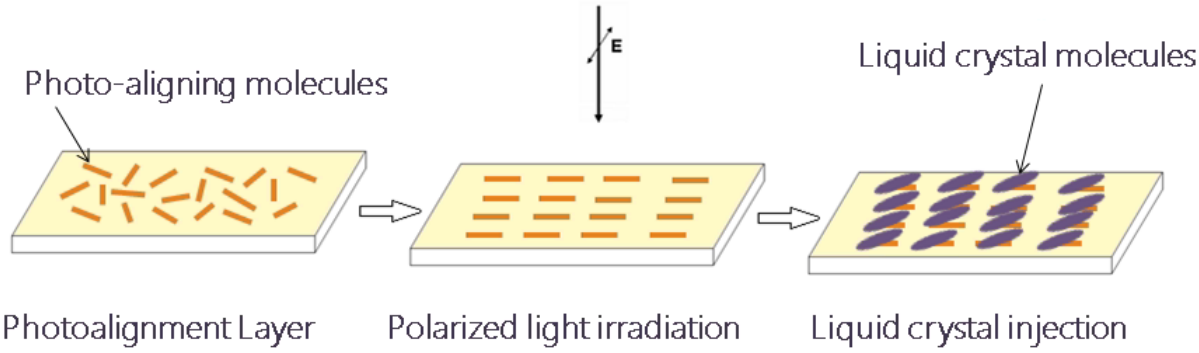

Figure 2.2: *The photoalignment process: A thin alignment layer containing the photoresponsive molecules are coated on the substrate surface. The coated layer is then exposed to a linear polarized UV light at suitable dose. When the photoalignment layer is brought in contact with the liquid crystal, the liquid crystal molecules adopt alignment perpendicular to or along the UV light polarization direction, depending on the nature of the photoresponsive material.*

tion, including Van der Waals, dipole-dipole, $\pi - \pi$ stacking, hydrogen bonding or steric interactions.

Most of the photoalignment materials consist of photoresponsive molecules whose strongest absorption direction is along their long molecular axis (see fig.(2.3)). However, there are also many materials whose strongest absorption direction is perpendicular to their long molecular axis. In general, photoalignment materials are considered to be the materials containing photosensitive species with angularly dependent light absorption. The molecules of most of them posses transition dipole moments oriented preferably along their long molecular axis.

Photoalignment processes and likewise photoalignment materials can be divided in several groups depending on the photo-induced mechanisms, photo-induced conformational changes of the photosensitive molecules or on the predominate photochemical reactions of the photosensitive groups [26].

Photochemical reactions can be classified as photoisomerization, photodecomposition, photocrosslinking, photodimerization, and a combination of photocrosslinking with photo decomposition or photoisomerization [26, 28]. Some examples are depicted in fig.(2.3) to fig.(2.6).

Photoisomerization phenomena is a reversible process in which *trans* - to *cis* isomerization takes place. Classical example of photo-induced isomerization is the one exhibited by the azo-dye molecules under exposure with linearly polarized UV light (see fig.(2.3)). Due to the multiple photo-induced *trans*- to *cis*-isomerization process the molecules' long axis initially parallel to the UV light polarization direction re-orients to perpendicular

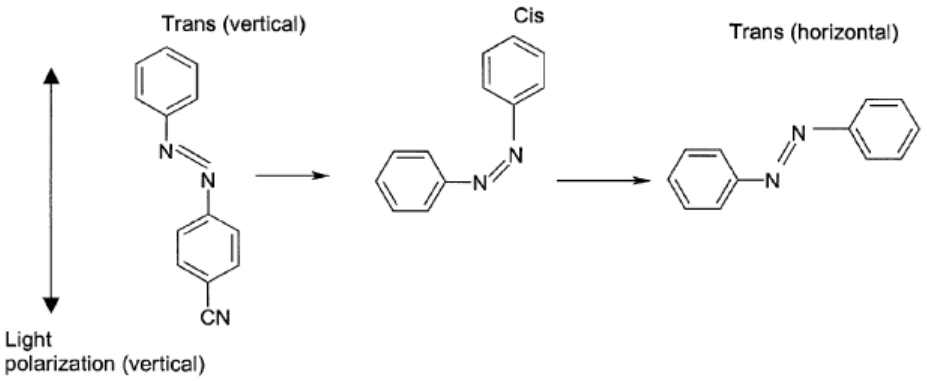

Figure 2.3: *Photo-induced trans − cis isomerization of azo-molecule under illumination with a linear polarized UV light. The trans−isomer, which long axis is initially parallel to the UV light polarization vector, undergoes multiple trans- to the cis- photoisomerization cycles resulting in re-orientation of the molecule long axis from the initially parallel to the light polarization vector position to perpendicular to it. [27].*

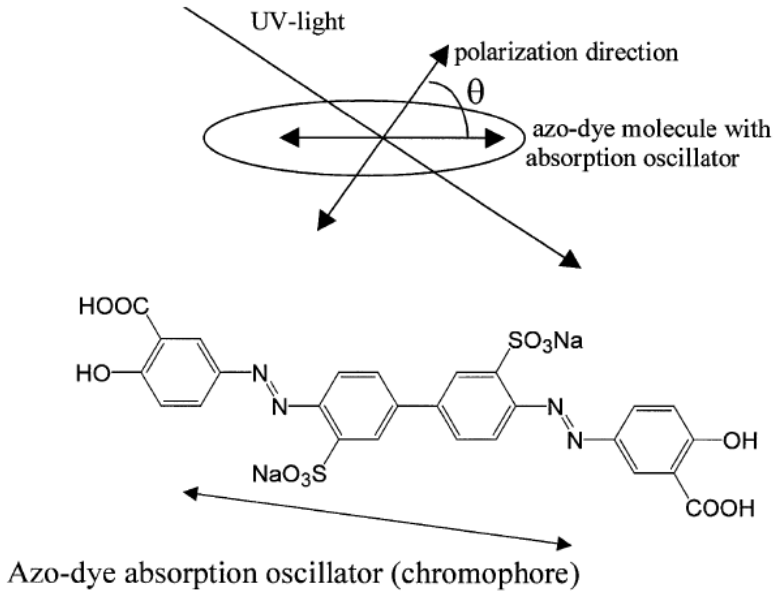

Figure 2.4: *The qualitative interpretation of the photo-induced order in photochemical stable azo-dye films. Above: the geometry of the effect; below: azo-dye molecule, having the absorption oscillator (chromophore) parallel to the long molecular axis [27].*

to it position [27, 29, 30]. The photo-isomerization transformation process of azo-dyes is employed for photoalignment of liquid crystals by azo-dye containing polymers and monolayers [28, 31].

Photoinduced reorientation mechanism observed in azo-dye molecules which align their long axes perpendicular to the UV light polarization direction is depicted in fig.(2.4) [30]. In this case the azo dye does't undergo *trans-* to *cis-* photoisomerization.

Photodecomposition of the alignment layer made of polymer has been applied to large

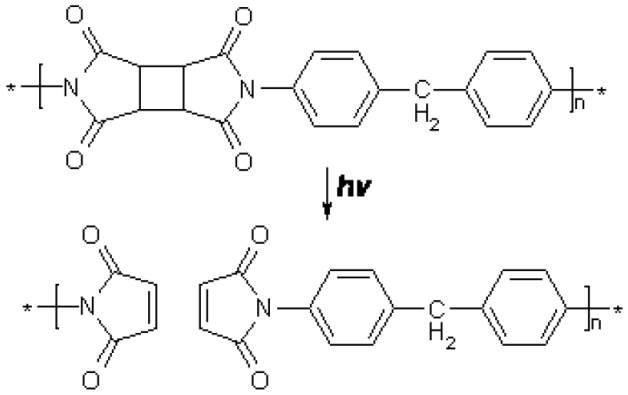

Figure 2.5: *Photodecomposition of polyimide backbone [32].*

number of different materials such as stable polyimides, polysilanes and polystyrene [32]. It was found that the absorption of linearly polarized UV light by the photodestructive parts of polyimides depends on their orientation with respect to the UV light polarization direction. The absorption will have a maximum (or minimum) when these parts lie parallel (or perpendicular) to the polarization direction of light. The anisotropic absorption results in anisotropic decomposition of the polymer chains, which changes the length distribution of the polyimide. The molecular structure of liquid crystal molecules and the liquid crystal/surface interaction will control the liquid crystal alignment [26, 32]. Photodestructive polyimides usually promote alignment with sufficiently high anchoring energy, $w^{\varphi} \geq 10^{-5} Jm^{-2}$.

Directed photocrosslinking process is used for producing photoalignment layers. In some side-chains polymers, radicals are generated by exposure to UV light. This process enables the connection of the polymer molecules in a new structure which possess certain anisotropy and thus enables photoalignment of the liquid crystals [33, 34]. The azimuthal anchoring energy of the liquid crystal alignment promoted by the photocrosslinked materials is usually in the range of $10^{-5} - 10^{-6} Jm^{-2}$.

Photodimerization is also used as a photoalignment method. It takes place when two photoreactive molecules have open bonds. These bonds absorb the UV light energy and dimerize when they are oriented parallel to the UV polarization direction [33, 34]. Photodimerization is now successfully employed as a photoalignment method in the Liquid

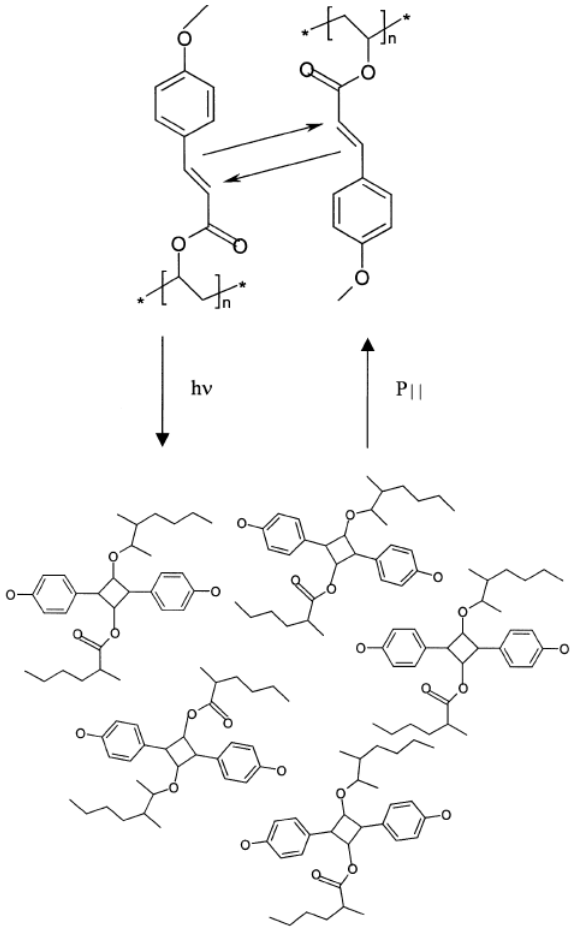

Figure 2.6: *Photo-dimerization of poly (vinyl cinnamate) - PVCi [26, 27].*

Crystal Displays (LCDs) industry (Sharp, Japan). Combinations of two photochemical reactions, like photocrosslinking and photodecomposition or photoisomerization, have been used to obtain proper photoalignment layers for liquid crystal devices [35].
Recently a diversity of new photoalignment materials and a variety of methods based on photoalignment technique have been developed and are still developing in order to meet the strong demand of the LCD industry. The main efforts of the researchers working in the area of the photoalignment of liquid crystals is to overcome certain deficiencies in the liquid crystal display operation such as, the narrow viewing angle, slow response by design, synthesis of new photoalignment materials and developing new techniques for photo-patterning of the alignment layers.
In this thesis, two different new series of photoreactive materials have been studied. New photoreactive materials having fluorine units (c.f. section 2.4.1) and novel azo containing thiophene based prop-2-enoates (c.f. section 2.4.2) has been investigated as photoalignment materials.

2.4.1 Photoreactive Materials Having Fluorine Units

The photoalignment ability for five different compounds of oxadiazoles with different substitutions have been investigated (see fig.(2.7) for their chemical structures).

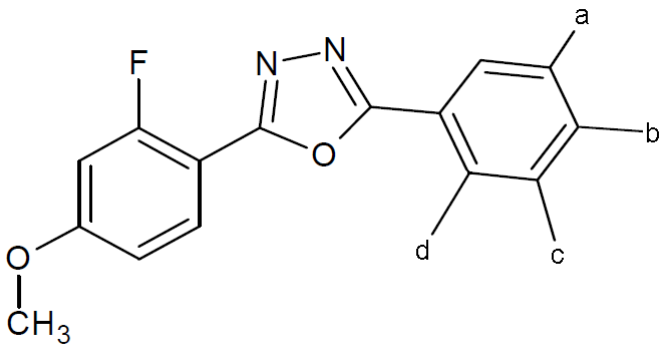

Figure 2.7: *Chemical structure of oxadiazoles used in this study. Notation a to d indicates the substitution of chlorine, bromine or fluorine.*

2.4.1.1 Experimental Procedure

Thin films of the investigated material deposited on the inner side of the glass substrates using the same method described in section 5.1. Experimental quartz substrates also were prepared in a similar way for light absorption study. The glass and quartz substrates covered with the photoresponsive film were exposed to linearly polarized UV light using standard USHIO light exposure equipment equipped with deep medium pressure mercury

lamp giving 3 mW/cm^2 linearly polarized UV light passing through polarizer and light filter cutting the light below 290 nm. The absorption spectra were determined using the quartz substrates as described in section 5.3. Conventional cells were prepared with the glass substrate. Nematic liquid crystal MLC 6873 - 100 ($\Delta\varepsilon > 0$) was filled at an isotropic phase in the cell via capillary action. The quality of the photoalignment was determined by polarizing optical microscope with crossed polarizers.

2.4.1.2 Results and Discussion

The compounds 4a (with the substitution of Cl and Br at positions a and c, respectively) and 4c (with the substitution of Cl at positions b)(c.f. fig.(2.7)) were found to be unable to promote uniform alignment of the nematic liquid crystal. Compound 4b (where the

Table 2.3: *Photoalignment promoted by oxadiazole compounds with F, Cl and Br substitutions and different position of the F atom(s) in the molecular structure obtained after 15 min of exposure with linear polarized UV light at 2 m W/cm^2.*

Materials	Photoalignment results	Molecular orientation
4a	No alignment	No alignment
4b	Good	perpendicular
4c	No alignment	No alignment
4d	Good	parallel
4e	Weak	perpendicular

fluorine is attached to position b) and 4d (where the fluorine is attached to the both sides of the molecule, i.e. positions a and c) were found to promote high quality planar alignment with preferred direction perpendicular and parallel to the light polarization direction, respectively. Furthermore, the compound 4e with substitution of two fluorine groups at positions c and d promoted weak planar alignment.
The results of this study are summarized in Table 2.3 and unambiguously demonstrate the importance of the molecular structure of the alignment material for the photoalignment ability of the material. Furthermore the position of the fluorine substitution in the molecular structure plays an important rule for the alignment quality as well as for the preferred direction of the photoalignment with respect to the light polarization direction.

2.4.2 Novel Azo Containing Thiophene Based Prop-2-enoates

Photo-reorientation of azo-dye molecules has been observed as a response to a linearly polarized UV light illumination. The probability of the absorption of light by azo-dye molecules is proportional to $\cos^2\theta$, where θ is the angle between the absorption oscillator of the azo-molecule and the polarization direction of the polarized light (c.f. fig.(2.4)) [27]. Consequently, the molecules which are parallel to the light polarization direction will most probably get an increase of energy and reorient themselves so that the direction of the absorption oscillator will tend to become perpendicular to the light polarization. As a matter of fact, this feature has been observed on alignment layers prepared from pure azo-dyes as well as from azo compounds, azo-dopants in polymer, and azo-polymers [36]. In the present thesis investigations have been performed on photoalignment layers prepared from materials with molecular structures based on azobenzene linkage (-N=N-), a lateral fluoro-substituents and a thiophene ring. The chemical structure of the materials is given in fig.(2.8).

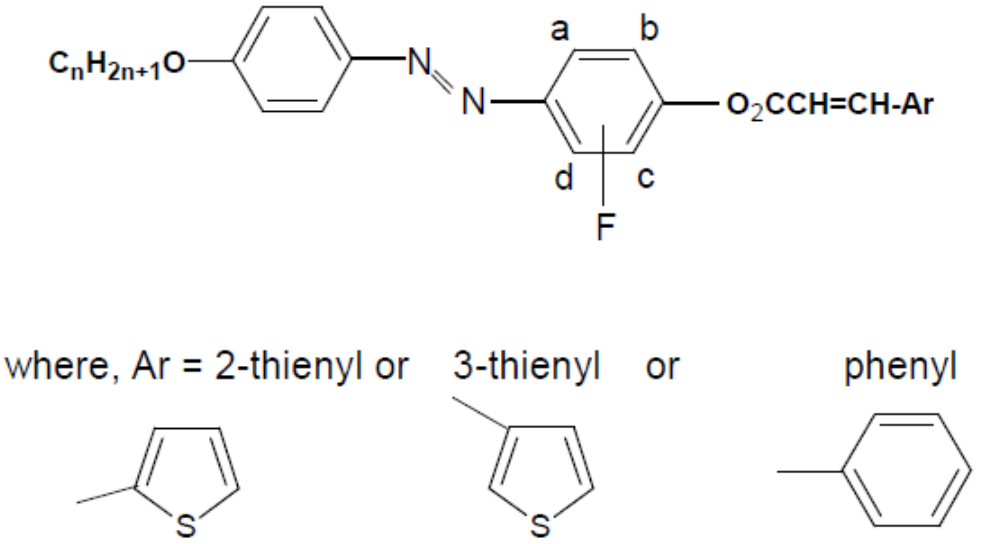

Figure 2.8: *Chemical structure of azo-containing thiophene-based prop-2-enoates.*

2.4.2.1 Experimental Procedure

Alignment layers have been prepared using the materials under investigation. Nematic liquid crystal cells were prepared as described in section (2.4.1.1) but with different light filter and exposure times. The absorption spectra were determined using ITO glass substrate coated with the photoalignment material as it is described in section 5.3.

2.4.2.2 Results and Discussion

The quality of photoalignment for one of these materials is demonstrated in fig.(2.9). The absorption spectra as illustrated in fig.(2.10) show that before irradiation with a linear polarized UV light, the absorption by the azo-dye layer is independent of the polarization of the light used in the measurements (curve 1). After irradiation by linearly polarized UV light for 15 min, however, the absorption of light shows polarization dependency. Absorption of light with its polarization direction parallel ($D_{\parallel}$) to the polarization direction of the UV light decreases (curve 2) whereas, absorption of light with its polarization direction perpendicular ($D_{\perp}$) to the UV light polarization direction increases (curve 3).

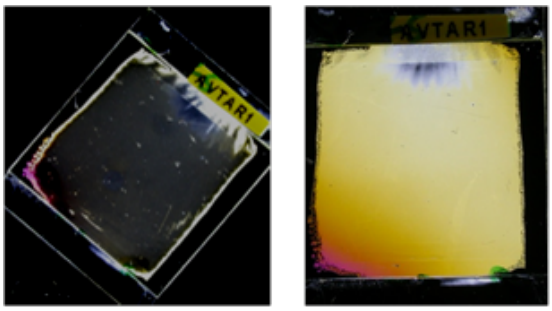

Figure 2.9: *Photomicrographs of the cell containing alignment layer made from 3-thienyl with mono fluoro-substituent in position 'b' ,i.e. C4:2F 3,3AE, observed between crossed polarizers. Excellent photoalignment is achieved with good dark state (on left side) and with good bright state (on right side).*

The quality of the alignment was found to be influenced by the number and disposition of the fluoro-substitutes. As well as the position of attachment of the terminal thiophene moiety.

Disposition of monofluoro-substitution on position '*c*' exhibited good alignment probably due to reduced steric hindrance, whilst the disposition of the fluoro-substituents across the long molecular axis (see position '*b*' and '*c*' or position '*a*' and '*d*' in the chemical structure) shows very good photoalignment since in this case the dipole associated with the two fluoro-substituents appears to impart an additive effect to the overall molecular polarizability.

Furthermore the position of the terminal thiophenes moiety contributes to improve the alignment quality where 3-substituted thiophenes exhibits superior alignment compared with their 2-substituted counterparts. In the 3-thienyl systems the sulfur atom contributes to molecular polarizability of the long molecular axis, whereas, in the 2-thienyl system the sulfur is disposed slightly off-axis and is able to contribute to the same effect.

The materials, that exhibited excellent photoalignment, are with 3-thienylacrylates bearing two lateral fluoro-substituents namely, C3:2,6F 3,3AE or C4:2,6F 3,3AE. Our study on these novel materials demonstrate the vital importance of the molecular structure of the

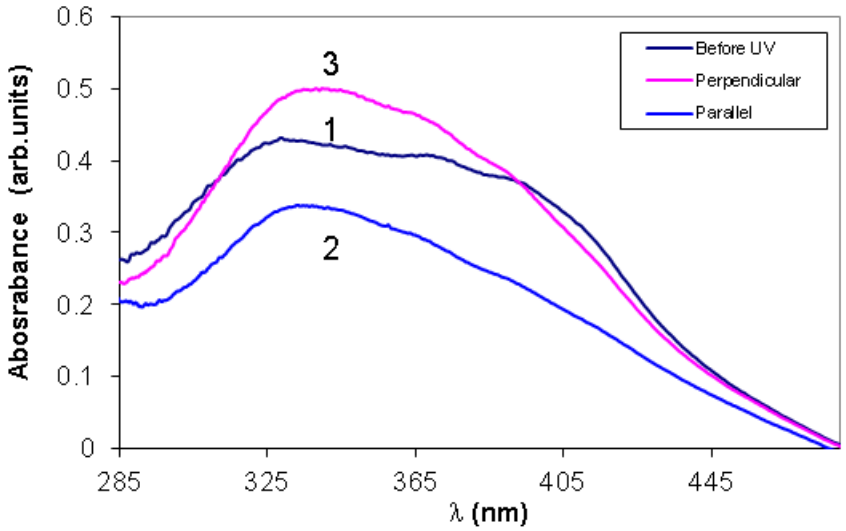

Figure 2.10: *Polarized absorption spectra for C4:2,6F 3,2AE, before (curve 1) and after irradiation with linearly polarized UV light (passing through 270 nm filter) parallel (curve 2) and perpendicular (curve 3) with respect to the main polarization axis for 15 minutes.*

aligning materials for the achievement of high quality photoalignment of nematic liquid crystals in LCDs with good thermal stability.

3 . Thickness Dependence of Anchoring Energy of a Nematic Cell

The surface contribution to the total energy of nematic liquid crystal cells is the anisotropic part of the surface tension. It appearers in the boundary conditions for the bulk differential equations. It is expected to be a local property independent of the bulk properties. However the actual nature and origin of the anchoring energy is still a matter of investigations. In the present thesis the dependence of the effective anchoring energy on the cell gap thickness, using a technique based on the relaxation time of an imposed deformation, has been investigated.

Let us consider a nematic liquid crystal cell with $\Delta\varepsilon < 0$, and uniform homeotropic field off alignment in the shape of slab of thickness d with the z-axis normal to the limiting surfaces at $z = \pm d/2$ and applied electric field $\mathbf{E} = E\mathbf{u}_z$. The sample under investigation has symmetric limiting surfaces i.e. $w_1 = w_2 = w$ and $\theta_1 = \theta_2 = \theta$. If the applied field is above the critical field for Freedericksz transition an elastic deformation will be induced reorienting the liquid crystal molecules towards the planar alignment. The evolution of the nematic tilt angle $\theta(z,t)$, when the applied electric field is removed, is governed by the balance between the electric torque and the viscous torque

$$k\frac{\partial^2\theta}{\partial z^2} = \eta\frac{\partial\theta}{\partial t}, \tag{3.1}$$

where k is the average elastic constant, and η is the rotational viscosity. In the frame work of Rapini-Papoular approximation the boundary conditions are

$$\pm\, k\frac{\partial\theta}{\partial z} + \frac{w}{2}\sin(2\theta) = 0, \tag{3.2}$$

at $z = \pm d/2$. In the linear limit equation (3.2) reduces to

$$\pm\, k\frac{\partial\theta}{\partial z} + w\theta = 0. \tag{3.3}$$

Assuming strong anchoring, i.e. $\theta(\pm d/2, t) = 0$; the complete solution of equation (3.1), taking the boundary conditions into account, will be

$$\theta(z,t) = \sum_{n=1}^{\infty} A_n \cos(a_n z)\, \exp(-t/\tau_n), \tag{3.4}$$

where the relaxation time τ_n is related to the wave-vector a_n by $\tau_n = (1/a_n^2)(\eta/k)$, and the wave vectors a_n are given by

$$a_n \tan(a_n d/2) = 1/b, \tag{3.5}$$

where $b = k/w$ is the extrapolation length.

3.1 Experimental Procedure

The alignment layer for this experiment has been prepared from SE1211 (Nissan Chem.). A set of nematic liquid crystal cells have been prepared with cell gap thickness ranging from about 1.5 μm up to 9 μm (c.f. section 5.1). The cell gap thickness measured using the procedure described in section 5.2. Nematic liquid crystal MLC 6608 ($\Delta\varepsilon < 0$, Merck) was injected into the empty cells in the isotropic phase (100°C). Electro-optics measurements carried out as described in section 5.4.

3.2 Results and Discussion

The measurements of the relaxation time τ versus the thickness of the cell showed an increasing dependence of τ on d. In the frame work of strong anchoring conditions τ depends on d according to the law

$$\tau = cd^2, \tag{3.6}$$

where $c = (\eta/\pi^2 k)$. The best fit of the experimental data to equation (3.6) obtained with $c = 5.2 \times 10^8 s/m^2$. The liquid crystal used in the experiment has $c = 1.1 \times 10^8 s/m^2$. This result indicates that the assumption of strong anchoring doesn't fit well for our system. Consequently, in the limit of large but finite w, we assumed an additional linear term i.e.

$$\tau = cd^2 + rd. \tag{3.7}$$

The parameters of the best fit of the experimental data to equation (3.7) were found $c = 6.4 \times 10^8 s/m^2$ and $r = -8.1 \times 10^2 s/m$. The negative value of r contradicts the assumption that the anchoring energy is thickness independent. Thus we conclude that the anchoring is not infinite, and not thickness independent.

The explanation to this thickness dependence is based on the selective adsorption of ions by the surfaces. The selective adsorption creates a surface electric field extends into the bulk to a distance λ_D (i.e. Debye length) and orients the liquid crystal molecules. The flexoelectric properties of the material is also to be considered (c.f. section 1.5.2). Assuming for τ the relaxation time measured in the experiment, the effective energy w_{eff} will be

$$w_{eff} = ka \tan(ad/2), \tag{3.8}$$

where $a = \sqrt{(\eta/k\tau)}$ and $\tau = (d/\pi)^2(\eta/k)$.
As discussed in section 1.5.2 the effective anchoring energy for a nematic cell, when the selective adsorption of ions and the flexoelectric effect are considered, is

$$w_{eff} = w + \frac{\sigma}{\varepsilon}\left(\frac{\Delta\varepsilon}{2\varepsilon}\lambda_D\,\sigma + 2\,e\right). \tag{3.9}$$

Using the data of the liquid crystal under investigation with the best fit parameter from equation (3.6), the values of the effective anchoring energy strength as a function of d have been evaluated using equation (3.8). The obtained values of $w_{eff}(d)$ have been fitted with equation (3.9) which is derived in a previous model.

Our investigation on the thickness dependence of the anchoring energy in the case

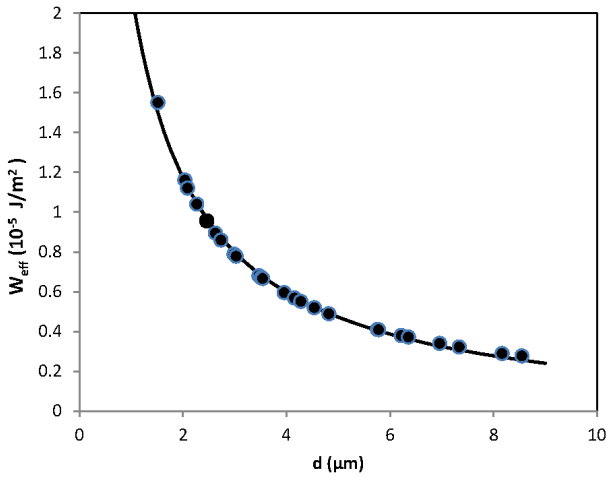

Figure 3.1: *Dependence of the surface anchoring energy, in the Rapini-Papoular approximation time versus the thickness of the cell, $\tau = \tau(d)$. Points are the experimental data evaluated by means of equation (3.8), with $\tau = c\,d^2$, with $c = 5.2 \times 10^8 s/m^2$. The continuous curve is the theoretical prediction of the model as discussed in the text.*

of alignment layers prepared from polyimide SE1211 (Nissan Chem.) showed excellent agreement with equation (3.9) as it is illustrated in fig.(3.1) considering the measured relaxation time in the form of $\tau = (d/\pi)^2(\eta/k)$. The parameters of the best fit are $\Sigma = 2.3 \times 10^{-4}$ C/m^2, $w = 2.8 \times 10^{-5}$ J/m^2 and $e = -8.3 \times 10^{-12}$ C/m.
From the additional two terms, in equation (3.9), which give rise from the surface electric field, we may conclude that both the purity of liquid crystal material and the high flexoelectric polarization are essential factors facilitate reducing the relaxation time by slight changes in the cell gap thickness. Thus by controlling liquid crystal characteristics, such as viscosity, dielectric anisotropy and elastic constants it is possible to control the anchoring properties and thus the electro-optic characteristics of LCDs.

4 . Anchoring (Alignment) Transition

When the solid substrate is in contact with liquid crystal molecules, the preferred direction of the substrate surface anisotropy is transferred to the liquid crystal via surface/liquid crystal interactions and the director tend to point to a certain direction reflecting the physical anisotropy of the surface. Changing the director orientation which is referred to as an anchoring (alignment) transition, can be induced by different means. Essentially there are two types of anchoring transitions: the anchoring transitions due to the liquid crystal/surface interaction or due to external forces. The surface effects mediated anchoring transitions are originating from the changes of the substrate physical properties by temperature, light or chemically triggered processes [4, 37–39]. External fields which may induce alignment transitions could be electric or magnetic fields as well as light. In this case the external factor has direct coupling to the liquid crystal bulk rather than with the liquid crystal/solid surface interface.

4.1 Light-Induced Anchoring Transition

Light-induced anchoring transition is a typical example of surface mediate transition. As mentioned previously, there is a group of liquid crystal materials whose molecules undergo *trans*- to *cis* photoisomerization (c.f. fig.(4.1)). The photoisomerization process may affect the bulk properties of the liquid crystal but also the character of the liquid crystal/ solid surface interaction, which in turn may cause an anchoring transition. A light command surface is one typical example of the light-induced reorientation of liquid crystal molecules from homeotropic to planar alignment under the action of the polarized light on azo-dye molecules with permanent one-side attachment to the inner substrate surface [29].

Another example of light-induced reversible anchoring transition is the selective absorption of *cis*-isomers generated by UV light illumination, on the polar solid surface. Such an absorption will cause transition of the initially planar alignment of nematic liquid crystal, in which are dissolved photoresponsive azo-molecules, to homeotropic due to the absorbed on the solid surface *cis*-isomers which have V-shape (c.f. fig.(4.2)) [35].

An irreversible transition from homeotropic to planar alignment is achieved by photodestruction of polyimides which have a backbone which promotes a planar alignment and

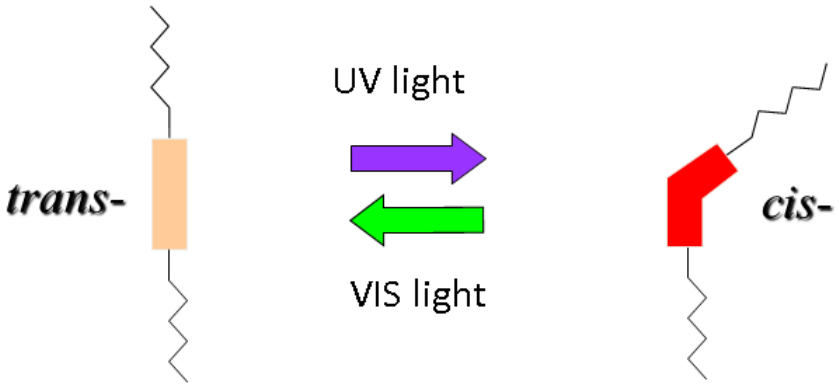

Figure 4.1: *Reversible photoisomerization, associated with: changes in the molecular shape (not always) and changes in the distribution of permanent dipole moments in the molecular structure.*

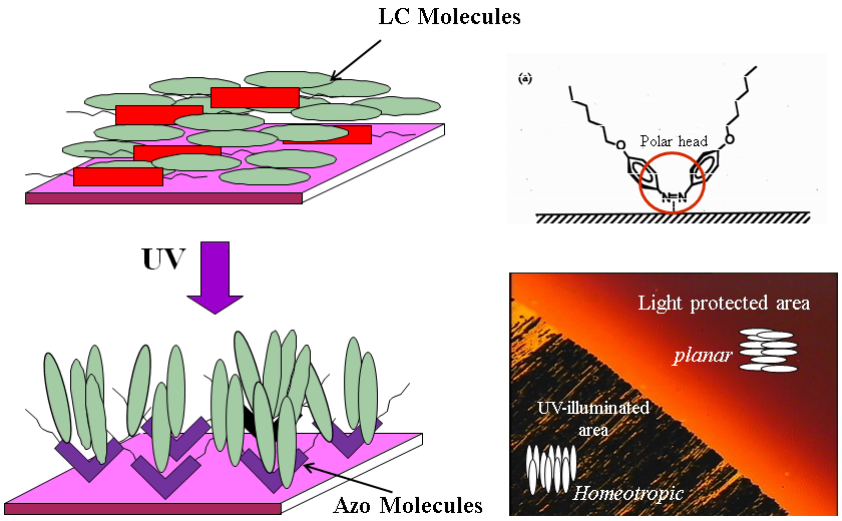

Figure 4.2: *Photo-induced alignment transition.*

side-chains (usually alkyl groups) which promotes homeotropic alignment. The illumination with UV light for a suitable time was found to break the bonds and reduce the size of the alkyl side-chains, which increases the polarity of the surface and hence increases the surface tension which results in homeotropic to planar transition [40, 41].

4.2 Light-Control of Pretilt Angle

The performance of the liquid crystal displays depends essentially on the liquid crystal alignment, either homeotropic, planar or tilted, and its characteristics such as anchoring strength and molecular pretilt with respect to the device substrates. There is a great demand on the liquid crystal alignment with certain pretilt, depending on the LCD mode, since the molecular pretilt strongly influences the electro-optical properties of liquid crystal displays such as the driving voltage, transmittance, viewing angle and response times. Strict control of the uniformity of liquid crystal alignment as well as the molecular pretilt and anchoring strength is of vital importance for the quality of the LCD performance.
In this thesis a previous theoretical model have been proved experimentally. This model considers an alignment surface prepared from two different components. One of the components promotes vertical alignment (VA) for nematic liquid crystals while the other promotes planar alignment (PA). These two components are distributed equally on the alignment surface and have anchoring strength proportional to their densities w_{VA} and w_{PA}, respectively. Then the surface energy of a nematic layer in contact with the polyimide alignment layer coated on the inner surface of the confining cell substrates will be [42]

$$f = -\frac{1}{2}\left\{w_{VA}\cos^2(\theta - \theta_{VA}) + w_{PA}\cos^2(\theta - \theta_{PA})\right\}, \tag{4.1}$$

where θ_{VA} and θ_{PA} are the corresponding pretilt angles for vertical and planar components respectively. The easy axis direction of liquid crystal molecules alignment is given by [42]

$$\theta_e = \arccos\sqrt{\frac{w_{VA}\cos[2\theta_{VA}] + w_e + w_{PA}\cos[2\theta_{PA}]}{2w_e}}, \tag{4.2}$$

where w_e is the effective anchoring strength [42]

$$w_e = \sqrt{w_{VA}^2 + 2w_{VA}w_{PA}\cos[2(\theta_{VA} - \theta_{PA})] + w_{PA}^2}, \tag{4.3}$$

$w_{VA} = (1-c)u_{VA}$, $w_{PA} = cu_{PA}$, c is the density of the orienting centers which are responsible for PA, u_{VA} and u_{PA} are connected with the interactions responsible for the alignment promoted by the orienting centers. According to this model, an abrupt transition from vertical to planar alignment can be achieved. Continuous control of the pretilt is possible by introducing small pretilt for one or both of the components.
The alignment layer for this experiment has been prepared from the polyimide SE1211

which in its structure has two important components: a rigid backbone and an alkyl side chains. The polyimide backbone alone promotes planar alignment of the nematic liquid crystals whereas the alkyl side chains are responsible for the vertical alignment which the nematic liquid crystal adopts in contact with the polyimide layer [43].

4.2.1 Experimental Procedure

The alignment layer for this experiment has been prepared from SE1211 (Nissan Chem.). Three different procedures have been used to prepare the alignment layer. The alignment layer for the first set of cells illuminated by linear polarized UV light source (6 mW/cm^2) [standard USHIO light exposure equipment with deep medium pressure mercury lamp]. The illumination done at normal incidence varying the exposure time. The second set has been rubbed manually (weak rubbing) unidirectionally before UV illumination. The third set has been rubbed manually (strong rubbing) unidirectionally before UV illumination. Two similar substrates were assembled together to form one cell as described in section 5.1. Nematic liquid crystal MLC 6608 ($\Delta\varepsilon < 0$) (Merck) was injected into the cells at isotropic temperature. Tilt angle measurements have been carried out using Mueller matrix spectrometer (c.f. section 5.5).

4.2.2 Results and Discussion

In this part the results of a study on an anchoring transition from vertical alignment to planar alignment using photoalignment technique in combination with the rubbing technique will be presented.

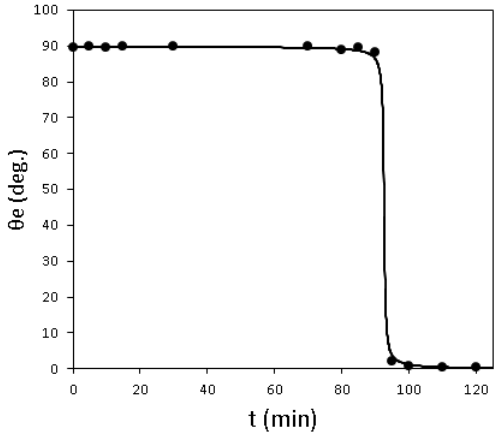

Figure 4.3: *The pretilt angle changes abruptly from* 89.8° *to* 0° *after 90 min of exposure. The circles represent the experimental data, the solid line represents the fitted curve of equation (4.2) with* $\theta_{VA} = 89.8°$. *The best fitting parameters are p = 0.00542 and u=1.*

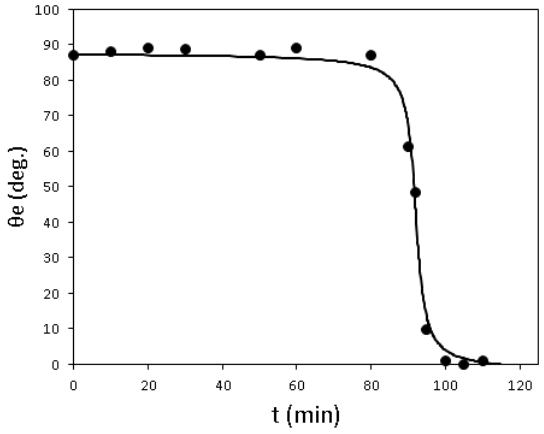

Figure 4.4: *Pretilt angle vs UV exposure time at weak rubbing condition. The circles represent the experimental data, the solid line represents the fitted curve of equation (4.2) with* $\theta_{VA} = 87.3°$*. The best fitting parameters are p = 0.0089 and u=0.25.*

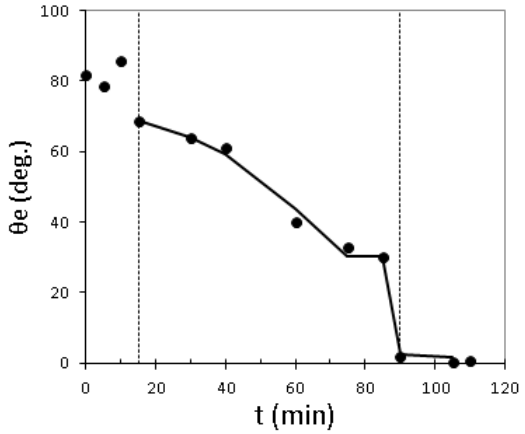

Figure 4.5: *Pretilt angle vs UV exposure time at strong rubbing condition. The circles represent the experimental data, the solid line represents the fitted curve of equation (4.2). The best fitting parameters are* $\theta_{VA} = 70.85 + 0.00379t^2$*,* $\theta_{PA} = 1 + \left[\frac{1}{1-0.000131t^2}\right]$*, p = 0.0091 and u=0.376.*

Let us consider now a liquid crystal alignment layer with two components acting simultaneously, one giving homeotropic alignment, i.e. vertical alignment, and planar alignment, respectively, without any pretilt. UV illumination for such polyimide results in bond breaking and hence cutting off the alkyl side chains, which increases the surface polarity as well as it reduces steric interaction between the liquid crystal molecules and therefore the surface/liquid crystal interactions now are promoting planar alignment. The suitable exposure time for this photo-induced VA to PA transition was found to be 100 min and it has the character of a first order transition (see fig.(4.3)). The density of the planar orienting centers (i.e. c) were assumed to be increasing linearly with the

exposure time i.e. $c = pt$. Using conventional rubbing technique applied on the alignment layer, before UV illumination, results in more inclination of the alkyl side chains and, moreover, orienting the rigid backbone in the rubbing direction. Hence after rubbing both anchoring components for VA and PA will have some pretilt. At weak rubbing this pretilt is expected to be very small whereas at strong rubbing it will be larger. At weak rubbing, after UV illumination of the rubbed alignment layer, the cell was found to give very sharp, but continuous, alignment transition from VA to PA (weak first order), or continuous and quite smooth transition (typical second order), at strong rubbing (c.f. fig.(4.4) and fig.(4.5)).

5 . Experimental Techniques

5.1 Cell Preparation

Conventional liquid crystal cells were used in the experiments performed in this work. They were prepared using glass substrates pre-coated with a thin transparent conductive film of Indium Tin Oxide (ITO) acting as electrode. Before preparation of the cells, the substrates were cleaned carefully. Standard cleaning process has been used to remove any possible contamination which may cause severe problems such as electric shortage, cell gap variation or non-uniform alignment of the liquid crystal layer.

In order to prepare a cell with certain type of alignment, a uniform thin film of alignment

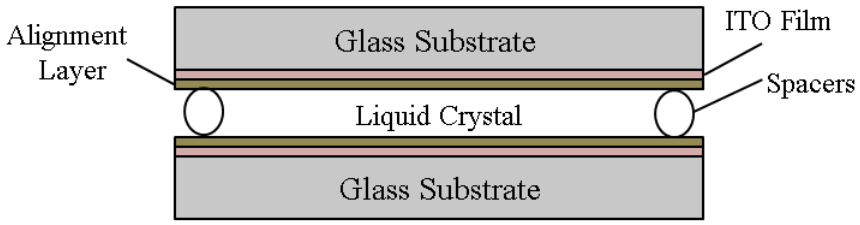

Figure 5.1: *Conventional sandwich type liquid crystal cell.*

material is deposited on top of the inner surface of each substrate of the cell. The most common way to prepare this film is to use the spin coating technique. The desired film thickness is obtained by controlling the speed revolution of the spinner and/or the concentration of the alignment material dissolved in a solvent. After drying and curing the thin film, the glass substrates are ready for further treatment or/and to be assembled as a sandwich cell. The further treatment could be a single, such a mechanical rubbing or UV light illumination, or a combination of them depending on the experiment requirement. The thickness of the cell gap has been adjusted by using spacers and chemically non-reactive glue are used for preparation of the sandwich cell. The spacers usually are mixed with the glue and placed outside the area of the electrodes. Two substrates are assembled together to get a small and uniform gap between the confining substrates (see fig.(5.1)). The sides of the assembled cell is sealed using UV glue. The liquid crystal is filled into the cell gap via capillary forces.

5.2 Cell Gap Measurement

The measurement of the thickness of an empty liquid crystal cell has been done by spectral interferometric method. I have used a LAMBDA POLYNOM UV-3100 spectrophotometer (300 -700 nm) and a SHIMADZU UV-visible-NIR light source (190 - 2000 nm) where the incident beam of light falls perpendicular to the cell. The wavelength of the transmitted light through the cell is scanned, the multipath interference peaks are recorded by the computer. In this method Fabry-Perot-type multipath interference peaks as a function of wavelength are used to determine the thickness of the cell. The empty cell works according to Fabry-Perot effect as optical resonator where the light is reflected and interfere with itself. The interference can take place if only the cell gap (d) equals an integer multiple of the wavelength λ

$$d = n.\frac{\lambda_1}{2}. \tag{5.1}$$

The next wave will fulfil the condition

$$d = (n+1).\frac{\lambda_2}{2}. \tag{5.2}$$

The difference between the two equations will give an equation to calculate the cell gap

$$\frac{\delta\lambda}{\lambda_1.\lambda_2} = \frac{1}{2.d}. \tag{5.3}$$

5.3 UV/vis Absorption Spectra

UV/vis absorption spectra, were determined using a LAMBDA POLYNOM UV-3100 spectrophotometer (300 -700 nm) and a SHIMADZU UV-visible-NIR light source (190 - 2000 nm) and performed on quartz substrates (or ITO glass substrates) coated with the photoalignment material. A polarizer was inserted in front of the light beam to measure the dichroic ratio.

5.4 Electro-optics Measurement

The electro-optic characteristics of the liquid crystal cells were measured by means of the set-up shown on fig.(5.2). The liquid crystal cell is inserted in a hot stage mounted on the turn table of the polarizing microscope. The cell is connected to a function generator with amplifier via resistance box and a suitable electric field is applied across the cell in order to induce out of plane transition from vertical to planar alignment. The microscope is connected to an optical detector. The electro-optic response of the cell and the driving voltage are displayed on Tektronix TDS 540 digital storage oscilloscope connected to the optical detector and the generator. Temperature control of the cell is done by using hot

stage. The electro-optic characteristics of the cells, such as rise and relaxation (fall) time and the character of the electro-optic response were directly measured and analyzed on the oscilloscope screen.

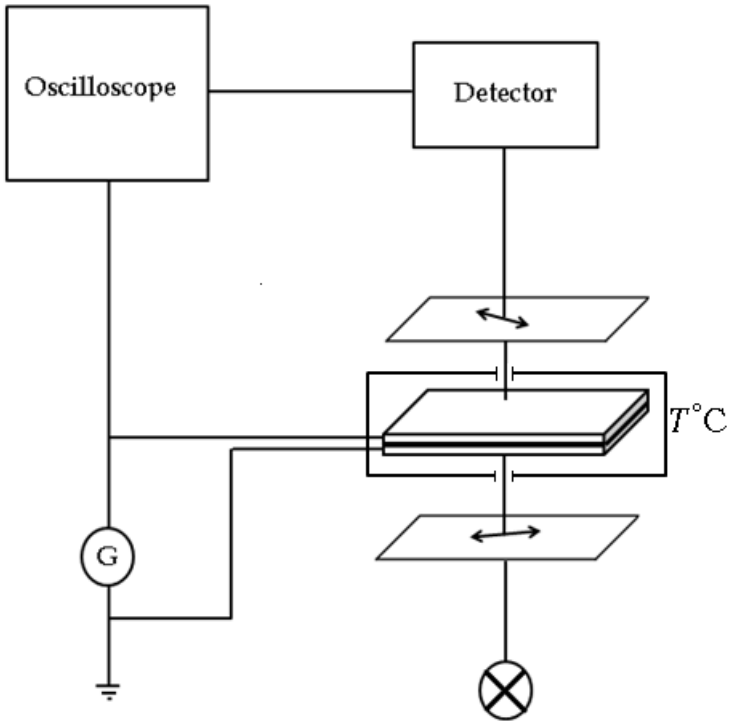

Figure 5.2: *Experimental setup for electro-optic measurements.*

5.5 Tilt Angle Measurement

Tilt angle measurements have been done using Mueller matrix spectrometer constructed by Ass. Prof. Ingolf Dahl [44]. The components of the spectrometer are illustrated

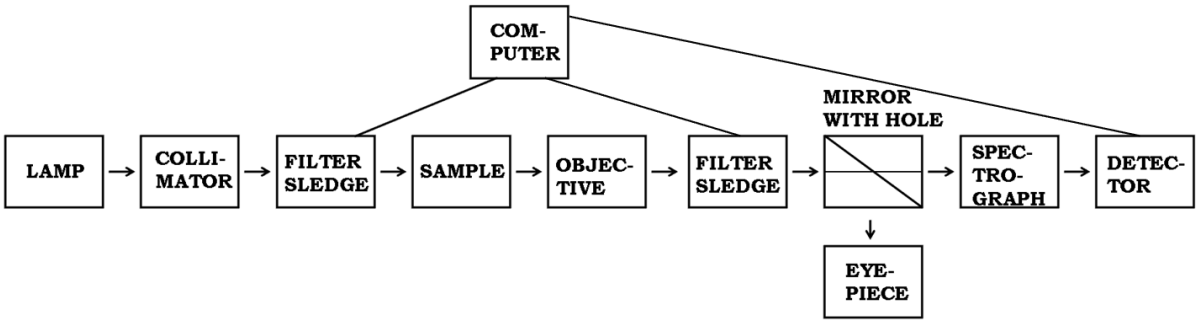

Figure 5.3: *The block scheme for the Mueller matrix spectrometer.*

in fig.(5.3). Light source (Xenon lamb) has been used to illuminate small area in the

cell (around spot with diameter 160 μm). Two Glan-Thompson prisms together with polarized-turning components on two step-motor controlled filter sledges are used (before and after the sample) to control the polarization of the light. To measure the intensity of the transmitted light, an Oriel Ms125 1/8 m Spectrograph with an Instaspec photodiode array (PDA) detection system have been used. The obtained spectrum is recorded by the computer and analyzed, using software written by Ass. Prof. Ingolf Dahl, to obtain tilt angle values.

6 . Conclusion

Liquid crystals have revolutionized the Information Technology during the last three decades. Their device application, the liquid crystal displays (LCDs) are today everywhere. They are important part of the computers, TV sets, measurement instruments, car boards, etc.

The important part of the LCD is the liquid crystal cell. Of vital importance for the performance of the liquid crystal cell is the liquid crystal material and its interactions with the cell substrates surfaces the liquid crystal is in contact with. Whereas the existing knowledge about the liquid crystals, in general, and nematic liquid crystals, in particular, is quite advanced, there is still lack of understanding of the liquid crystal/solid surface interaction and their impact on the liquid crystal cell performance. This interaction is the mechanism behind the alignment of the liquid crystal in a sandwich cell such as the one of the LCD. The alignment characteristics of the liquid crystal such as pretilt and anchoring strength are of vital importance for the performance of the LCD. The control of these characteristics is very important in the LCD industry. Without such a control it will be impossible to have reliable LCDs with high quality.

Mechanically rubbed polyimide layers are widely used today as alignment layers for LCDs. The rubbing process, however, is generating mechanical defects and electrostatic charges, which may worsen the LCD performance and damage the TFTs of the active matrix driving system. Moreover, with the increase of the size of LCDs and the need for patterned alignment of the liquid crystal, other non-contact methods for liquid crystal alignment enabling the full control of the alignment characteristics, such as photoalignment, become very attractive.

The major goal of the work presented in this thesis was to reveal the relations between the alignment ability of different photoresponsive materials in relation to their molecular structure. Such information is of vital importance for the design and synthesis of photoalignment materials and it is forwarded now to the chemists, we are collaborating with, to design and synthesize new photoalignment materials based on the gained in this thesis knowledge.

It is well known, that the main obstacle for generating fast moving images in LCDs is the slow response time of the nematic liquid crystals used. Partial success is achieved by a proper tailoring the liquid crystal characteristics, such as viscosity, dielectric anisotropy

and elastic constants. Although the progress in this direction, such a tailoring of the liquid crystal material parameters has also its limits. It seems that another possible way for shortening the response times is to tailor the alignment characteristics of the liquid crystals, such as pretilt and anchoring strength. It should be pointed out here that this approach is not easy at all.
Another important issue treated in this thesis is whether the anchoring strength of the liquid crystal is only a surface properties. Our study proved that the anchoring is also a liquid crystal bulk properties, i.e. depends on the ionic concentration in the liquid crystal bulk and their adsorption on the substrate surface. The anchoring strength also depends on the flexoelectric coefficients and dielectric anisotropy of the liquid crystal. The result of this study open the possibility for controlling the anchoring strength by controlling not only the surface physical characteristics but also tailoring the liquid crystal materials' parameters.
The last but not the least goal of the thesis is to study some of the important mechanisms behind the generation of a pretilt in the alignment of nematic liquid crystals. The experimental results of this study confirmed the conclusions of our theoretical model. According to this model, the alignment surface containing uniformly distributed VA and PA centers with surface energy proportional to their densities results in an abrupt VA to PA transition with the increase of the concentration of PA centers, i.e. there is no possibility to generate any pretilt due to the fact that both VA and PA components have no pretilt, which was predicted by our theoretical model. However, by introducing some small pretilt of one or both alignment components, by means of mechanical rubbing of the alignment layer for instance, a small pretilt will be generated so that the VA to PA transition becomes continuous and, depending on the rubbing strength, the pretilt could be controlled in wide range. Hence, breaking the surface symmetry by employing mechanical treatment is an important factor in the achievement of a continuous control of the pretilt.

To summarize shortly the importance of the results obtained in this thesis work:

- revealing some of the important relations between the molecular structure of the alignment material and its photoalignment ability the design of appropriate photoalignment materials becomes feasible.

- revealing the important factors for realizing of an efficient control over the alignment characteristics, pretilt and anchoring strength, which enables the reduction of the response times of the electro-optic response in LCDs (fast switching) and of the required driving voltage, resulting in an improvement of the LCDs' performance.

Acknowledgements

First and foremost, my deepest gratitude is expressed to my supervisor Professor Lachezar Komitov for giving me the opportunity to join his group and for his continuous guidance and encouragement with all patience through my entire PhD program and thesis work.

Also I am extremely indebted to Dr. Gurumurthy Hegde for leading me through my first steps in the Clean Room and the laboratories area, and giving me the secrets of LC alignment technology. I am also thankful to his suggestions, useful discussions and continuous support.

My deepest appreciation and gratitude is extended to Professor Giovanni Barbero for his guidance, suggestions and endless help during the theoretical analysis.

I would like to extend my gratitude to Ass. Prof. Ingolf Dahl for careful guidance during using Mueller Matrix Spectrometer, and for his help to solve various technical problems.

I am thankful to Professor Dag Hanstorp for his critical reading and indispensable comments.

I also want to acknowledge University of Khartoum, Sudan for supporting me financially.

I would like to thank Dr. Gunnar Andersson for always being available for help and keeping the instruments working.

I am thankful to Jan-Åke Wiman for his useful designs. Thanks should also go to Bea, Johanna, and Maria at the administration for their help. I also offer my thanks to my colleague Omaima Abubakr for her kind help and useful discussion, and to all those who contributed directly or indirectly in this work.

Finally, I am most grateful to my parents, my uncles, and my siblings for their continuous support and encouragement without which this work could not have been under taken.

Bibliography

[1] E. P. Prriestley, Peter J. Wojtowicz, and Ping Sheng, *Introduction to Liquid Crystals*, Plenum Press, New York and London, 1979.

[2] P.G. De Gennes and J. Prost, *The Physics of Liquid Crystals*, Clarendon Press, Oxford, 1993.

[3] Lev M. Blinov, *Structure and Properties of Liquid Crystals*, Springer, 2011.

[4] L. M. Blinov and V. G. Chigrinov, *Electrooptic Effects in Liquid Crystal Materials*, Springer, 1996.

[5] Frederic J. Kahn, Gary N. Taylor, and Harold Schonhorn, *Proceedings of The: IEEE.*, **61**, 7 (1973).

[6] Vladimir G. Chigrinov, *Liquid Crystal Devices: Physics and Applications*, Artech House, Boston London, 1999.

[7] G. Barbero and L. R. Evangelista, *An Elementary Course on The Continuum Theory For Nematic Liquid Crystals*, World Scientific,Singapore, 2001.

[8] A. A. Sonin, *The Surface Physics of Liquid Crystals*, Gordon and Breach Publishers, Luxembourg, 1995.

[9] G. Barbero and G. Durand, *Journal of Applied Physics*, **67**, 2678 (1989).

[10] G. Barbero and G. Durand, *Journal of Physics France*, **51**, 281 (1990).

[11] A. L. Alexe-Ionescu, G. Barbero and A. G. Petrov, *Physicscal Review E*, **48**, R1631 (1993).

[12] E. Jakeman and E.P. Raynes, *Physics Letters*, **39A**, 1 (1972).

[13] H.-M. Wu, J.-H. Tang, Q. Luo, Z.-M. Sun, Y.-M. Zhu, Z.-H. Lu and Y. Weia *Appl. Phys. B*, **62**, 613 (1996).

[14] Y. B. Kim et al., *Mol. Cryst. Liq. Cryst.*, **262**, 89 (1995).

[15] J. C. Jung, K. H. Lee, B. S. Sohen, S. W. Lee, M. Ree, *Macromol. Symp.*, **164**, 227 (2001).

[16] Masahito OH-E, Doseok Kim, and Y. R. Shen, *Analytical Sciences*, **17**, i805 (2001).

[17] Z.Huang, Ch.Rosenblatt, *APL*, **86**, 011908 (2005).

[18] Wei-Yen Wu, Chen-Chen Wang, and Andy Ying-Guey Fuh1, *Optics Express* , **16**, 17131 (2008).

[19] J. L. Janning, *Appl. Phys. Lett.*, **21**, 173 (1972).

[20] L. A. Goodm, J. T. Mcginn, C. H. Anderson and F. Digernimo, *IEEE*, **ED-24**, 795 (1977).

[21] K. Hiltrop and H. Stegemeyer, *Mol. Cryst. Liq. Cryst.*, **49**, 61 (1978).

[22] L. M. Blinov and Usp. Khimii, *Mol. Cryst. Liq. Cryst.*, **52**, 1263 (1983).

[23] Ghanshyam P. Sinha, Bing Wen, and Charles Rosenblatt, *Applied Physics Letters*, **79**, 16 (2001).

[24] Tatsutoshi Shioda, Bing Wen, and Charles Rosenblatt, *Phys. Rev. E* , **67**, 041706 (2003).

[25] Xiangyi Nie, Ruibo Lu, Haiqing Xianyu, Thomas X. Wu, and Shin-Tson Wu, *Journal OF Applied Physics*, **101**, 103110 (2007).

[26] Kohki Takatoh, Masaki Hasegawa, Mitsuhiro Koden, Nobuyuki Itoh, Ray Hasegawa and asanori Sakamato, *Alignment Technologies and Applications of Liquid Crystal Devices*, Taylor and Francis, London and New York, 2005.

[27] Vladimir Chigrinov, V. M. Kozenkov, and H. S. Kwok, *Optical Applications of Liquid Crystals*, Ed. Bristol, MA:Inst.Physics, 201 (2003).

[28] Vladimir Chigrinov, Vladimir Kozenkov, and Hoi-Sing Kwok, *Photoalignment of Liquid Crystalline Materials: Physics and Applications*, John Wiley and Sons, Ltd, (2008).

[29] Kunihiro Ichimura, Yasuzo Suzuki, Takahiro Seki, Akira Hosoki, and Koso Aoki, *Langmuir*, **4**, 1214 (1988).

[30] Vladimir Chigrinov, Sergey Pikin, Andrey Verevochnikov, Vladimir Kozenkov, Maxim Khazimullin, Jacob Ho, Dan Ding Huang, and Hoi-Sing Kwok, *Physical Review E*, **69**, 061713 (2004).

[31] O. V. Yaroshchuk, A. D. Kiselev, Yu. Zakrevskyy, T. Bidna, J. Kelly,3 L.-C. Chien, and J. Lindau, *Physical Review E*, **68**, 011803 (2003).

[32] Lyudmyla Vretik et al., *Liquid Crystalline Organic Compounds and Polymers as Materials of the XXI Century* , 153 - 189 (2011).

[33] M. O'Neill and S. M. Kelly *J. Phys. D: Appl. Phys.*, **33**, R67 (2000).

[34] O. Hyun Sung, S. Hyun Cho, W. Gun Kim, K. Gook Song, S. Hyon Paek, and J. Young Lee, *Macromol. Symp.*, **29**, 249 (2007).

[35] K. Ichimura, Y. Akita, H. Akiyama, K. Kudo, and Y. Hayashi, *Macromolecules*, **30**, 903 (1997).

[36] Oleg Yaroshchuk and Yuriy Reznikov, *J. Mater. Chem.*, **22**, 286 (2012).

[37] L. Komitov, J. Yamamoto and H. Yokoyama , *J. Appl. Phy*, **89**, 7730 (2001).

[38] G. Ryschenkow and M. Kleman, *J. Chem. Phys.*, **64**, 404 (1976).

[39] P. Jagemalm and L. Komitov, *Liq. Cryst.*, **23**, 1 (1997).

[40] Shaoqin Gong, Jerzy Kanicki, Lan Ma, and John Z. Z. Zhong *Japanese Journal of Applied Physics*, **38**, 5996 (1999).

[41] Kang-Wook LEE, Alan LIEN, James H. STATHIS and Sang-Hyon PAEK, *Japanese Journal of Applied Physics*, **36**, 3591 (1997).

[42] L. Komitov, G. Barbero, I. Dahl, B. Helgee and N. Olsson, *Liquid Crystals*, **36**, 747 (2009).

[43] Himali D. Jayathilake et al., *J. Chem. Phys.*, **125**, 064706 (2006).

[44] Ingolf Dahl, *Measurement Science and Technology*, **12**, 1938 (2001).